Toward Solving the Unstable Linear Fredholm Equation of the First Kind: A New Procedure Called the Adsorption Stochastic Algorithm (ASA) and Its Properties

Piotr A. Gauden

N. Copernicus University, Department of Chemistry, Physicochemistry of Carbon Materials Research Group, Gagarin Street 7, 87-100 Toruń, Poland

Piotr Kowalczyk

Department of Chemistry, Faculty of Science, Chiba University, 1-33 Yayoi, Inage, Chiba 263, Japan

Artur P. Terzyk*

N. Copernicus University, Department of Chemistry, Physicochemistry of Carbon Materials Research Group, Gagarin Street 7, 87-100 Toruń, Poland

Received December 20, 2002. In Final Form: March 20, 2003

The paper consists of three main parts. In the first, a new "adsorption stochastic algorithm" (called ASA) for solving the unstable linear Fredholm integral equation of the first kind is proposed. In this program, some procedures of estimating the relative minimum in one dimension are tested. The newly developed algorithm is applied in the second part for reconstructing some pore size distribution functions (monomodal and multimodal). Moreover, the influence of a random noise on the stability of the solution of the inverse problem is studied. In the third part, the experimental verification of the above-mentioned method is presented. The results calculated by ASA are compared with those obtained by applying advanced regularization CONTIN and INTEG algorithms. It is shown that the developed ASA method always provides stable and very similar results to Tikhonov's regularization method. Moreover, the ASA computations obtained for the Nguyen and Do local isotherms as the kernel are very similar to the results calculated by the most sophisticated regularization density functional theory software. Summing up, the method can be very useful for evaluating the pore size distribution from experimental data.

I. Introduction

At present, there is a large and growing literature on the numerical solution of integral equations; even several monographs have appeared by now.[1] One reason for the sheer volume of this activity is that there are many different kinds of equations, each with many different possible pitfalls, and therefore many different algorithms have been proposed to deal with a single case.

Although, while composing a new algorithm, authors usually have taken into consideration the shortcomings of the previous ones, an ultimate procedure for the solution of the linear Fredholm integral equation of the first kind has not been elaborated yet. Thus, new efforts are needed to improve the methods of the analysis of this problem. First, the new proposed method should be faster than those previously proposed and should enable one to attain approximately the same accuracy (it should be reproduced so that the original multipeak and complicated "unknown" function are obtained with excellent accuracy, while omitting the appearance of some artificial peaks). Second, that formulation of a minimization problem should exclude an unphysical value of unknown and evaluated function (i.e., strong oscillations, a negative value of a probabilistic distribution function, and so on). Moreover, the program code of the algorithm should be simple, short, and easy for application for the wide group of scientists.

This article is organized as follows. In the first section, we describe some recent methods concerning the numerical solution of the linear Fredholm integral equation of the first kind. Since the procedure described in the current study has been developed for solving the problems in the field of adsorption studies (obviously it can be also applied elsewhere), we focus on the methods widely applied in this field. They will be treated as reference ones. Next, the way of formulation of the problem of nonquadratic minimization and the procedure of its solving (i.e., discretization of distributions) are presented. In this part, the new algorithm, the "adsorption stochastic algorithm" (ASA) is described in detail. The third section is devoted to the results of some numerical experiments. Then we compare the pore size distributions (PSDs) evaluated from experimental data using the ASA, INTEG, and CONTIN methods. Finally, we present conclusions.

II. Theory of the Fredholm Linear Equation of the First Kind

The general linear equation may be written in the following form:[1−3]

$$h(x)f(x) + \int_c^d K(x,y)f(y)\,dy = g(x) \qquad (c \le y \le d) \text{ and } (a \le x \le b) \quad (1)$$

* To whom correspondence should be addressed. Phone: (+48) (056) 611 4371. Fax: (+48) (056) 654 2477. E-mail: aterzyk@chem.uni.torun.pl.

(1) (a) Morozov, V. A. *Methods for Solving Incorrectly Posed Problems*; Springer: Berlin, 1984. (b) Tikhonov, A. N.; Arsenin, V. Y. *Solutions of Ill-Posed Problems*; Winston & Sons: New York, 1997.

10.1021/la0270441 CCC: $25.00
Published on Web 04/18/2003

where known functions $h(x)$, $K(x,y)$, and $g(x)$ are assumed to be bound and usually to be continuous. If $h(x) \equiv 0$, the equation is of the *first kind*; if $h(x) \neq 0$, the equation is of the *second kind*; if $h(x)$ vanishes somewhere but not identically, the equation is of the *third kind*. In the present paper, we consider only the linear Fredholm integral equation of the first kind. In one dimension, it has the following generic form:[4]

$$\int_c^d K(x,y)f(y)\,dy = g(x) \tag{2}$$

where the functions $K(x,y)$ (the *kernel*) and $g(x)$ (the *right-hand side*) are known ones, at least in principle, while $f(y)$ is an unknown, sought function. In many, but not all, practical applications of eq 2, the kernel $K(x,y)$ is given exactly by the underlying mathematical model, while the right-hand side $g(x)$ typically consists of measured quantities, that is, $g(x)$ is only known with a certain accuracy and only in a finite set of points $s_1, s_2, ..., s_m$. Equation 2 is the analogue to the matrix equation

$$\mathbf{g} = \mathbf{K}\cdot\mathbf{f} \tag{3}$$

the solution of which is $\mathbf{f} = \mathbf{K}^{-1}\cdot\mathbf{g}$, where $\mathbf{K}^{-1}$ is the inverse matrix. Like eq 2, eq 3 has the unique solution whenever $\mathbf{g}$ is nonzero (the homogeneous case with $\mathbf{g} = 0$ is hardly ever useful) and $\mathbf{K}$ is invertible.

1. The Solution of Adsorption Integral Equations. The analysis of physical adsorption data has become a standard method of assessment of the energetic and structural heterogeneity of solid adsorbents.[5−12] The theoretical description of adsorption on heterogeneous solids is usually interpreted by the superposition of adsorption on independent homogeneous sorption sites and/or in pores with the same widths. Therefore, in the past 25 years considerable progress in the analysis of these quantities has been achieved due to the appearance of advanced numerical methods for solving the unstable linear Fredholm integral equation of the first kind (eq 2). A universal procedure for the characterization of solid adsorbents connected with choosing numerical methods for the evaluation of structural and geometric heterogeneity does not exist. A comprehensive review of different methods of the solution of the integral equation (the condensation approximation (CA), very popular due to its simplicity; regularization methods; and non-negative least-squares (NNLS) methods) can be found (for example) in three basic monographs devoted to adsorption.[5,12,13] On the other hand, estimating the distribution function from eq 2 is a well-known ill-posed (or "incorrect") problem, which is manifested by the fact that there exists an infinitely large set of possible solutions, all satisfying eq 2 with the accuracy of the experimental error. In other words, all solutions may have arbitrary large deviations from each other (and from the true solution) but they can fit the experimental data well at the same time.

To select a meaningful solution of the unstable linear Fredholm integral equation of the first kind from a set of all possible solutions, a number of the most famous and successful algorithms have been described by different authors: HILDA (heterogeneity investigated by a Loughborough distribution analysis),[14] ALINDA (Adamson−Ling distribution analysis),[15] CAEDMON (computed adsorptive energy distribution in the monolayer),[16] CAESAR (computed adsorption energies using singular value decomposition (SVD) analysis result),[15,17] EDCAIS (energy distribution computation from adsorption isotherm utilizing the smoothing spline functions),[18] REMEDI,[19] SAIEUS (solution of adsorption integral equation using splines),[20] INTEG (solution of adsorption integral equation),[21] IRA (improved regularization algorithm),[22] EM (expectation maximization),[23] CONTIN,[24] REG,[25] and others (for example, the methods based on Stietljes and Laplace transforms,[5] the methods based on the Fourier transform,[5,26] or the Rudziński−Jagiełło method[5,27]).

It is very interesting that the majority of the abovementioned methods have been proposed for the evaluation of the energy distribution functions. The INTEG algorithm and the CONTIN package are two methods also being successfully used for the estimation of the pore size distribution of adsorbents. Therefore, the main assumptions of both methods are shortly described in the next section, taking mainly the minimization problem into consideration.

2. Tikhonov Regularization Method. As was reported by Tikhonov,[1b,3] most of the linear Fredholm integral equations of the first kind are characterized by ill-posed character, which is manifested by the fact that even small changes in the data cause large changes in the solution. Since the function $g(x)$ is not known accurately, we should state the problem as

$$\int_c^d K(x,y)f(y)\,dy = g(x) + \epsilon(x) \qquad (c \le y \le d) \text{ and } (a \le x \le b) \tag{4}$$

where $\epsilon(x)$ represents an error term and is an arbitrary

(2) Phillips, D. L. *J. Assoc. Comput. Mach.* **1962**, *9*, 8.
(3) Tikhonov, A. N. *Dokl. Akad. Nauk USSR* **1943**, *39*, 195.
(4) Press, W. H.; Teukolsky, S. A.; Vetterling, W. T.; Flannery, B. P. *Numerical Recipes in Fortran*; Cambridge University Press: Cambridge, 1992.
(5) Rudziński, W.; Everett, D. H. *Adsorption of Gases on Heterogeneous Surfaces*; Academic Press: New York, 1992.
(6) *Equilibria and Dynamics of Gas Adsorption on Heterogeneous Solid Surfaces*; Rudziński, W., Steele, W. A., Zgrablich, G., Eds.; Elsevier: Amsterdam, 1997.
(7) Wojsz, R. *Characteristics of the Structural and Energetic Heterogeneity of Microporous Carbon Adsorbents Regarding the Adsorption of Polar Substances*; UMK: Toruń, 1989 (in Polish).
(8) Jankowska, H.; Świątkowski, A.; Choma, J. *Active Carbon*; Ellis Horwood: New York, 1991.
(9) Do, D. D. *Adsorption Analysis*: *Equilibria and Kinetics*; Imperial College Press: London, 1998.
(10) Gregg, S. J.; Sing, K. S. W. *Adsorption, Surface Area and Porosity*; Academic Press: London, 1982.
(11) Dubinin, M. M. In *Progress in Membrane and Surface Science*; Cadenhead, D. A., Ed.; Academic Press: New York, 1975; Vol. 9, p 1.
(12) Jaroniec, M.; Madey, R. *Physical Adsorption on Heterogeneous Solids*; Elsevier: Amsterdam, 1988.
(13) Cerofolini, G. F.; Re, N. *Riv. Nuovo Cimento Soc. Ital. Fis.* **1993**, *16*, 1.
(14) House, W. A.; Jaycock, M. *Colloid Polym. Sci.* **1978**, *256*, 52.
(15) Koopal, L. K.; Vos, C. H. W. *Colloids Surf., A* **1985**, *14*, 87.
(16) (a) Ross, S.; Morrison, I. D. *Surf. Sci.* **1975**, *52*, 103. (b) Sacher, R. S.; Morrison, I. D. *J. Colloid Interface Sci.* **1979**, *70*, 153.
(17) Vos, C. H. W.; Koopal, L. K. *J. Colloid Interface Sci.* **1985**, *105*, 183.
(18) Brauer, P.; Fassler, M.; Jaroniec, M. *Thin Solid Films* **1985**, *123*, 245.
(19) Koopal, L. K.; Vos, K. *Langmuir* **1993**, *9*, 2593.
(20) Jagiełło, J. *Langmuir* **1994**, *10*, 2778.
(21) v. Szombathely, M.; Brauer, M.; Jaroniec, M. *J. Comput. Chem.* **1992**, *13*, 17.
(22) Mamleev, V. Sh.; Bekturov, E. A. *Langmuir* **1996**, *12*, 441.
(23) Stanley, B. J.; Białkowski, S. E.; Marshall, D. B. *Anal. Chem.* **1993**, *65*, 259.
(24) (a) Provencher, S. W. *Comput. Phys. Commun.* **1982**, *27*, 213. (b) Provencher, S. W. *Comput. Phys. Commun.* **1982**, *27*, 229. (c) Provencher, S. W. *CONTIN Users Manual*, Version 2; Max-Planck-Institut für Biophysikalische Chemie: Göttingen, Germany, 1984.
(25) Hansen, P. C. *Numer. Algorithms* **1994**, *6*, 1.
(26) LumWan, J. A.; White, L. R. *J. Chem. Soc., Faraday Trans.* **1991**, *87*, 3051.
(27) Vilieras, F.; Michot, L. J.; Bardot, F.; Cases, J. M.; Francois, M.; Rudziński, W. *Langmuir* **1997**, *13*, 1104.

function except for some condition with respect to the size of $\epsilon(x)$, such as $|\epsilon(x)| \leq M$ or $\int_a^b \rho(x)\epsilon^2(x)\,dx \leq \bar{M}$, $\rho(x) > 0$ (where M and/or $\bar{M}$ can be treated as the maximum experimental error (upper limit of the error value) and/or the maximum average overall error[2] (i.e., experimental and numerical)). Instead of the unique solution of eq 4, we get the Γ family of solutions. The real problem then is to pick out the true solution $f(y)$ of the family of function Γ. This can be done without any more information about the problem given in eq 4. However, we can assume that the true solution $f(y)$ is a reasonably smooth function. With this assumption, the best approximation to $f(y)$ we can choose is probably the function $f_s(y) \in \Gamma$, which is the smoothest in some sense. So the smoothness of the unknown distribution function $f(y)$ was used as an additional minimizing condition for the stabilization of the solution. On the basis of that assumption, the classical least-squares functional defined as[3]

$$\text{Minimize } (g(x) - \int_c^d K(x,y)f(y)\,dy)^2 \quad \text{with respect to } f(y) \quad (5)$$

should be replaced by the functional[1]

$$\text{Minimize } (g(x) - \int_c^d K(x,y)f(y)\,dy)^2 + \Psi[f(y)] \text{ with respect to } f(y) \quad (6)$$

where $\Psi[f(y)]$ is an additional term (i.e., penalty function[28]) for the stabilization of the solution. In the well-known Tikhonov regularization method, the term can be written in alternative forms[2,3,21] where a regularization parameter (λ) is additionally introduced. The choice of the optimal value of this parameter is crucial for searching for the $f(y)$ function. A very low value of the regularization parameter (i.e., the assumption of low values of experimental error) gives rise to spurious peaks, while a value that is too high oversmooths the $f(y)$ function. A detailed description of strategies for finding the optimal λ can be found elsewhere.[21,29−31] We want to point out that the Tikhonov method is not computationally simple and the obtained solution strongly depends on the proper choice of the regularization parameter.

III. Problem Formulation

The problem of solving the integral Fredholm equation of the first kind (eq 2) may be replaced by a classical nonlinear minimization problem with constraints. So, in general, we can define the expression describing the global adsorption isotherm in a discreet form.[16,22,23,32] Thus, in the current studies eq 2 can be rewritten as follows:

$$\Psi_t(p_j) = \int_{z_{min}}^{z_{max}} g_{theor}(z,p_j)f(z)\,dz \cong \sum_{i=1}^{N} w_i g_{theor}(z_i,p_j) \quad i = 1, 2, ..., N \quad j = 1, 2, ..., M \quad (7)$$

where z describes the heterogeneity of an adsorbent related to one of the properties of the porous medium (as a rule, of the adsorption energy or structure); $f(z)$ is the distribution function of a parameter z (z_{min} is the smallest and z_{max} is the largest value of a property considered in the analysis); $g_{theor}(z,p)$ is the discreet form of a local function (i.e., kernel) describing, for example, the adsorption process (via pressure, p) in homogeneous (the same pore width and/or energy) pores (in other words, this quantity describes the "local adsorption isotherm"); and N is the number of weight vectors $\bar{\mathbf{w}}$ (it can be associated with the number of the local functions). Thus, we are defining the objective function (i.e., fitness function, functional):

$$\text{Minimize } \Omega(\bar{\mathbf{w}}) = \sum_{j=1}^{M}[\Psi_t(p_j) - \sum_{i=1}^{N} w_i g_{theor}(z_i,p_j)]^2 \text{ with respect to } \bar{\mathbf{w}} = (w_1, w_2, ..., w_N) \in R^N \quad (8)$$

where M is the number of adsorption isotherm points. In other words, the proposed procedure finds the weights of participation of local functions (i.e., a discrete form of the integral equation kernel $g_{theor}(z,p)$) in relation to the experimentally measured global function $\Psi_t(p)$. Recently, Nguyen and Do[32] projected the numerical algorithm of the minimization of the objective function defined by eq 8. Do's algorithm is based on the minimization procedure proposed by Nedler and Mead (i.e., the simplex method).[4] This method belongs to the classical nongradient optimization methods, and for this reason the solution of such a procedure can be trapped in local minima of the objective function. As reported by Do et al.,[32] such a type of algorithm can be successfully applied for the estimation of pore size distribution from a single adsorption isotherm with the assumption of successive minimization in one dimension. On the basis of Do,[32] we decided to apply the relaxation method in the proposed new ASA algorithm (the minimization procedure is a successive optimization in one dimension (i.e., to determine only one element from vector $\bar{\mathbf{w}}$)). First, we define a general programming problem as follows:

$$\text{Minimize } \Omega(\bar{\mathbf{w}}) = \begin{cases} \sum_{j=1}^{M}(\Psi_t(p_j) - \sum_{i=1}^{N} w_i g_{theor}(z_i,p_j))^2 & \text{if } \bar{\mathbf{w}} \in \Xi \cap S \\ \sum_{j=1}^{M}(\Psi_t(p_j) - \sum_{i=1}^{N} w_i g_{theor}(z_i,p_j))^2 + \sum_{i=1}^{\mathscr{N}} \Phi_i \delta_i & \text{otherwise} \end{cases} \quad (9)$$

where

$$\begin{cases} \delta_i = 1 & \text{if constraint } i \text{ is violated} \\ \delta_i = 0 & \text{if constraint } i \text{ is satisfied} \end{cases} \quad (10)$$

with the very fundamental normalization condition of weights $\sum_{i=1}^{N} w_i = 1$, where $\bar{\mathbf{w}} \in \Xi \cap S$. The feasible search space Ξ was assumed to be outside the defined N-dimensional rectangle. Here $\mathscr{N}$ is the number of constraints, $\Omega(\bar{\mathbf{w}})$ is the penalized objective function, and Φ_i is a constant imposed for the violation of the constraint i. The set $S \subseteq R^N$ defines the search space, and the set $\Xi \subseteq R^N$ defines a feasible search space. The search space S is defined as an n-dimensional rectangle in R^N (domains of variables defined by their lower and upper bounds)

$$0 \leq l(i) \leq w_i \leq u(i) \qquad 1 \leq i \leq N \quad (11)$$

(28) Olivier, J. P.; Conklin, W. B. *Proceedings of the First International Symposium on the Effect of Surface Heterogeneity in Adsorption and Catalysis on Solids, Kazimierz Dolny, Poland, 1992.*

(29) Hansen, C. *SIAM Rev.* **1992**, *34*, 561.
(30) Puziy, A. M.; Volkov, V. V.; Poznayeva, O. I.; Bogillo, V. I.; Shkilev, V. P. *Langmuir* **1997**, *13*, 1303.
(31) Cherkashinin, G. Y.; Ismakaev, M. K.; Bubnov, A. V.; Drozdov, V. A. *Inverse Probl.* **2000**, *16*, 1421.
(32) (a) Nguyen, C.; Do, D. D. *Langmuir* **2000**, *16*, 1319. (b) Do, D. D.; Do, H. D. *Langmuir* **2002**, *18*, 93.

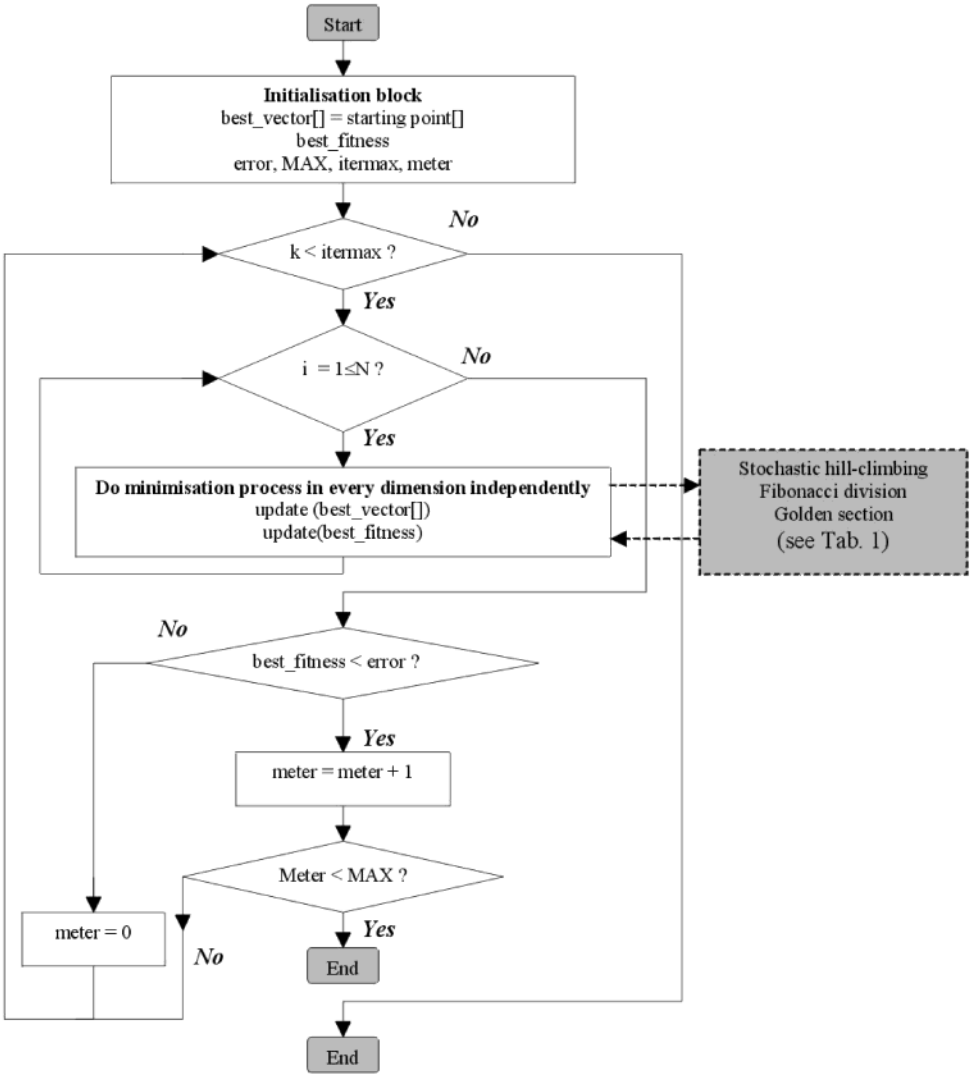

Figure 1. The flowchart of the ASA algorithm. Legend: best_vector, $\bar{\mathbf{w}} = (w_1, w_2, ..., w_N)$ for the starting point (the uniform distribution of weights is assumed); best_fitness, the parameter characterizing the fitness of the global theoretical isotherm to the experimental one; itermax, maximum number of iterations; error, accuracy of the fitness; and MAX, the critical number of iterations according to the condition best_fitness < error.

It is important that the defining of the minimization problem should prevent one from receiving unphysical solutions (i.e., negative values of the distribution function $f(z)$, unphysical oscillations of the distribution function $f(z)$, and so on). Up till now, we have defined only a minimization problem of the functional $\Omega(\bar{\mathbf{w}})$ but we do not say anything about constructing minimization procedures.

To extract $f(z)$ from a measured global adsorption isotherm, we can use genetic algorithms, evolutionary algorithms, simulated annealing, taboo search, deterministic algorithms (i.e., the simplex strategy of Nelder and Mead, the strategy of Hook and Jeeves, and so on), gradient methods (i.e., the simple gradient method and so on), and hybrid methods.[4,33−39] All the powerful techniques mentioned above minimize all unknown variables simultaneously. This new algorithm can be assigned to the so-called one-point strategy methods. Major steps of the ASA algorithm are shown on a flowchart in Figure 1. The main idea of such a minimization procedure is successive optimization in one dimension (i.e., to determine only one element from vector $\bar{\mathbf{w}}$). As an example, we can consider the problem of recovering the true continuous distribution function $y = f(z)$ (Figure 2). First, the linear Fredholm integral equation of the first kind is discretized (see Figure 2A). Following that, one estimates the best value of the objective function (with the assumption of uniform distribution of weights) and defines the control parameters of the algorithm (i.e., meter, required accuracy, the number of iterations, and the termination condition; see the initialization block in Figure 1). Now, the main minimization loop is executed. The algorithm starts the minimization process of the functional (eq 9) assuming the uniform distribution of weights (part B of Figure 2). So, only optimizing the first elements of optimization variables, the $\bar{\mathbf{w}}$ vector first carries out the

(33) Michalewicz, Z.; Fogel, D. *How to Solve It*: *Modern Heuristics*; Springer-Verlag: Berlin, 2000.
(34) Michalewicz, Z. *Genetic Algorithms + Data Structures = Evolution Programs*; Springer-Verlag: Berlin, 1996.
(35) Schwefel, H. P. *Evolution and Optimum Seeking*; John Wiley: Chichester, 1995.
(36) Golberg, D. E. *Application of Genetic Algorithms*; WNT: Warszawa, 1995 (in Polish).
(37) Arabas, J. *Lecture Notes on Evolutionary Computation*; WNT: Warszawa, 2001 (in Polish).
(38) Findeisen, W.; Szymanowski, J.; Wierzbicki, A. *The Theory and the Computational Methods of Optimalisation*; PWN: Warszawa, 1980 (in Polish).
(39) *Handbook of Evolutionary Computation*; Bäck, T., Fogel, D., Michalewicz, Z., Eds.; Oxford University Press: New York, 1996.

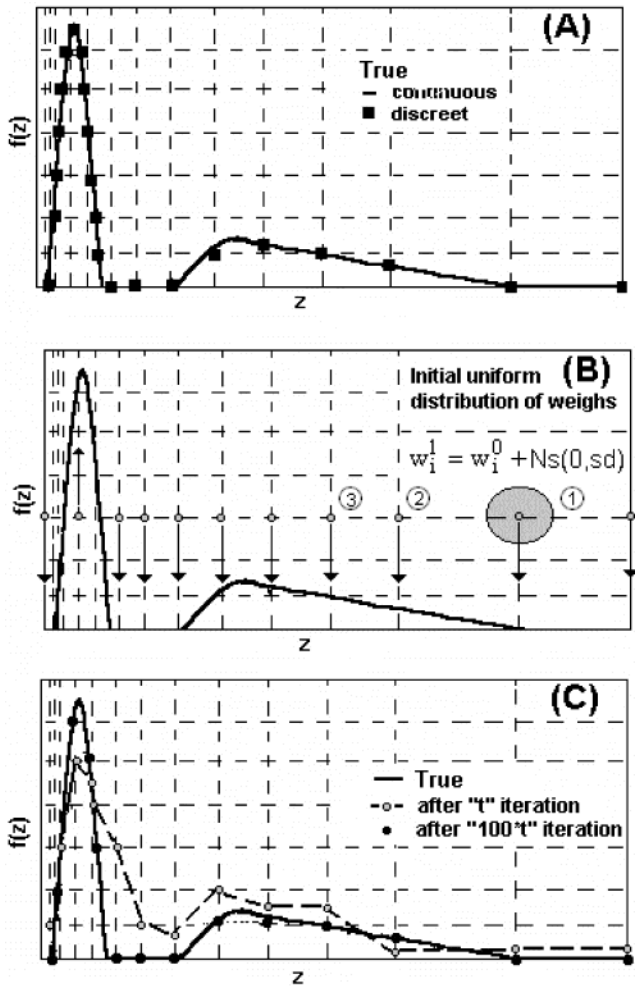

Figure 2. Schematically shown progress of the minimization process performed by the ASA algorithm (see the text and Figure 1 for details). The simple iterated hill-climber algorithm (ISHC) for which the climbing process is created by the Gaussian mutation technique (normal noise, Ns(0,sd) with specified mean and standard deviation) is considered.

optimization. Once w_1 is determined, w_2 is then optimized next until w_N has been considered. In other words, the weights are successively updated. The algorithm updates both the best vector and the best value of the objective function using minimization procedures in one dimension (the two-step termination condition is checked). The process is then repeated (the algorithm stops) until no further significant change in the functional is observed (when the same solution is repeated MAX times and/or the required accuracy of the fitness is achieved, Figure 1). It is shown (Figure 2C) that the initial weight distribution successively approaches the true solution during iterations.

IV. Numerical Examples and Experimental Data

In this part, we present the results of some numerical experiments. Nguyen and Do[32,40] developed a new method (ND) for the evaluation of pore size distribution from adsorption data. The local isotherms generated by applying the model proposed recently by those authors[32,40] are considered. The procedure is based on the combination of the Kelvin equation and the statistical adsorbed film thickness. A proposed methodology is similar to that used a couple of decades ago to describe the mesopore size distribution. A significant difference is that Do and coworkers take into account the enhancement in the n-BET/BET (Brunauer−Emmett−Teller) equation constant due to the stronger dispersive forces in smaller pores as well as the enhancement in the pressure exerted by molecules occluded in the pore. The most important feature of this method is the possibility of analysis of the structural heterogeneity of porous solids without separate approaches to micro- and mesopores.

In agreement with the following assumptions, Do and co-workers[32,40] proposed extending the well-known n-BET/BET and Kelvin theories describing the adsorption process on the flat surfaces and condensation in mesopores, respectively, to the adsorption in micropores. The fractional filling of a pore (i.e., local adsorption isotherm, assumed with $g_{theor}(z,p)$ in eqs 8 and 9) having half-width d is defined as the ratio of the thickness $t(p,H)$ to the maximum allowable physical half-width which is

$$\Theta_{ND}(p,H) = \begin{cases} \left(\dfrac{t(p,H)}{H/2}\right) & \text{for } p < p^* \\ 1 & \text{for } p \geq p^* \end{cases} \qquad (12)$$

where $(H/2) = (d - \sigma_{ss}/2)$; σ_{ss} is the collision diameter of a surface atom equal to 0.34 nm for C atoms on a carbon surface; p is the equilibrium pressure and the saturation vapor pressure, respectively; p^* is the critical pressure at which the pore filling occurs, and it is evaluated from the solution of the modified Kelvin equation (assuming that p is equal to p^*),

$$d - t(p,d) - \frac{\sigma_{ss}}{2} - \frac{\gamma v_m \cos\theta}{RT \ln(p/p_s)} = 0 \qquad (13)$$

where γ is the liquid surface tension; v_m is the liquid molar volume; θ is the liquid−solid contact angle; R is the universal gas constant; T is temperature; and p_s is the saturation vapor pressure. On the other hand, the statistical thickness of the adsorbed layer (occurring in eqs 12 and 13) is equal to

$$t(p,d) = t_m \frac{c_B z_B}{(1 - z_B)} \times \left[\frac{1 + (n_B b/2 - n_B/2) z_B{}^{n-1} - (n_B b + 1) z_B{}^{n} + (n_B b/2 + n_B/2) z_B{}^{n+1}}{1 + (c_B - 1) z_B + (c_B b/2 - b/2) z_B{}^{n} - (c_B b/2 + b/2) z_B{}^{n+1}}\right] \qquad (14)$$

t_m is the thickness of a single layer of the adsorbate equal to $a_m/S_{BET} = (v_m/N_{av})^{1/3}$ (a_m is the BET monolayer capacity, S_{BET} is the area of the flat surface, and N_{av} is Avogadro's number); $b = \exp[\Delta\epsilon/RT]$; $\Delta\epsilon$ is the excess of the evaporation heat due to the interference of the layering on the opposite wall of pores (usually it is smaller than 3 kJ mol^{-1} (i.e., $\Delta\epsilon \approx 2.2$ kJ mol^{-1})); $c_B = c_{s,B} \exp[(Q_{pore}(d) - Q_{surface}(d \rightarrow \infty))/RT]$; $c_{s,B}$ is the BET coefficient for adsorption on a "flat" surface; $Q_{surface}(d \rightarrow \infty)$ and $Q_{pore}(d)$ are the adsorption heat on a flat surface and in pores, respectively (the heat of adsorption is equal to the minimum of the potential function taken with a minus sign); $z_B = p/p_s$; n_B is the number (noninteger) of statistical monolayers of adsorbate molecules, and its maximal value for the given d is equal to $(d - \sigma_{ss}/2)/t_m$. The supplementary details of the Nguyen−Do model and experimental verification for

(40) (a) Nguyen, C.; Do, D. D. *Langmuir* **1999**, *15*, 3608. (b) Nguyen, C.; Do, D. D. *Carbon* **2001**, *39*, 1327. (c) Do, D. D.; Nguyen, C.; Do, H. D. *Colloids Surf., A* **2001**, *187−188*, 51. (d) Do, D. D.; Do, H. D. *Appl. Surf. Sci.* **2002**, *7821*, 1. (e) Do, D. D.; Do, H. D. *Langmuir* **2002**, *18*, 93. (f) Nguyen, C.; Do, D. D. *J. Phys. Chem. B* **2000**, *104*, 11435.

various adsorbent systems have been widely described elsewhere.[32,40,41]

Summing up, the solution of eq 7 (the kernel $g_{theor}(z,p)$ is assumed as the ND local adsorption isotherm (eq 12), the pore size distribution $f(z)$ is assumed as $f(H)$ and is unknown) is a well-known "ill-posed" problem. Therefore, knowing the adsorption isotherms in individual pores of different dimensions one can deal again with the linear Fredholm equation of the first kind. To verify the proposed algorithm, a number of numerical experiments with the postulated model distributions were carried out. Therefore we investigated (a) the influence of the shape of $f(H)$ on PSD reconstruction, (b) the influence of random noise on the stability of a solution of the inverse problem, and (c) the influence of the choice of the algorithm (ASA, CONTIN, INTEG) applied for the characterization of geometric heterogeneity of adsorbents on PSDs calculated from experimental data.

Moreover, to explain the details of the ASA algorithm, nitrogen adsorption data measured for the commercial activated carbon Norit ROW 0.8 SUPRA (Norit, Amersoort, Holland) are investigated. Nitrogen adsorption isotherms were measured using an ASAP 2010 volumetric adsorption analyzer from Micromeritics (Norcross, GA) at liquid nitrogen temperature (77.5 K) in the relative pressure range from about 10^{-6} up to 0.999. Before the measurements, the samples were outgassed for 2 h at the temperature of 473 K (the same measurement conditions were applied for all the samples studied in this paper). Norit ROW 0.8 SUPRA is mainly microporous (i.e., the "external" surface is negligibly small compared to the total apparent surface area). Since the shape of the measured low-temperature nitrogen adsorption isotherm suggests that microporosity is dispersed over a relatively wide range of pore widths, those adsorption data should provide a PSD curve that spreads over a relatively wide range of pore diameters.[41c,42]

1. The Choice of a Procedure for Estimating the Relative Minimum in One Dimension Implemented in ASA. In the ASA program, the well-known procedures for estimating the relative minimum in one dimension can be used; for example, stochastic hill-climbing (ISHC, the simple iterated hill-climber algorithm for which the climbing process is created by the Gaussian mutation technique);[33] golden section, 1st variant (GS1st);[38] Fibonacci division (FD);[35] parabolic interpolation and Brent method (PIBM);[4] golden section, 2nd variant (GS2nd);[4] one-dimensional search with first derivatives (ODSFD);[4] and grid method (GM).[38] All minimization routines applied with ASA give very similar values and shapes of the pore size distributions (see Figure 3). Moreover, time of the evaluation (CPU time) of the PSD differs significantly (Table 1, Figures 4 and 5). The value of the critical determination coefficient ($DC_{critical}$) characterizing the fitness of the global theoretical isotherm (calculated from the Nguyen−Do model) to the experimental data is assumed as greater than 0.999 (in this case, it is the stopping condition of the ASA algorithm, but in the next part, some more rigorous conditions are assumed). CPU time in the current studies is the total time required for generating the local adsorption isotherm and the evaluation of the unknown pore size distribution function. The data presented here are obtained on a 1.1 GHz processor laptop (240 MB of RAM).

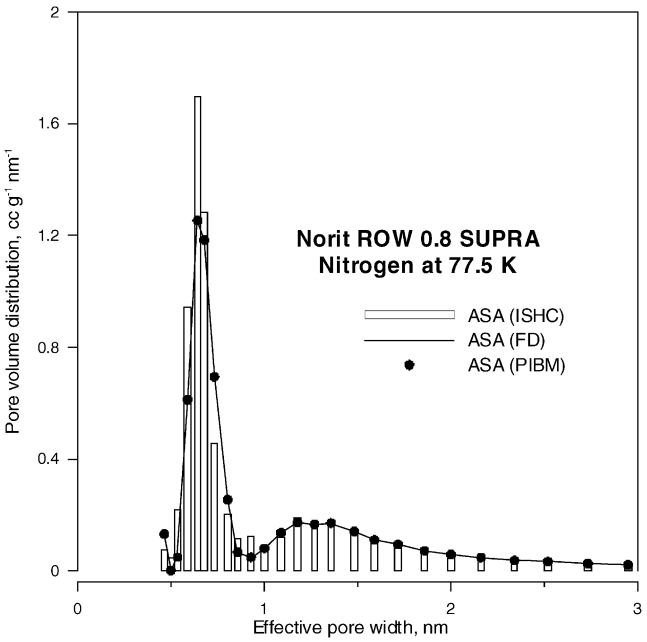

Figure 3. Pore size distributions of the activated carbon Norit ROW 0.8 SUPRA calculated using Nguyen and Do local isotherms in a discreet form of the unstable linear Fredholm integral equation of the first kind. The comparison of the one-dimension strategy implemented in ASA; only three cases from all presented in Table 1 are considered (the number of iterations is limited by the critical value of the determination coefficient assumed as equal to 0.999).

Table 1. Comparison of the Time of Computation of One-Dimension Strategies Implemented in ASA[a]

model	number of iterations	CPU execution time, s
ISHC	41	85
GS1st	48	156
FD	48	477
PIBM	48	61
GS2nd	48	88
ODSFD	48	85
GM	51	3298

[a] The low-temperature nitrogen adsorption data on the carbon Norit ROW 0.8 SUPRA are studied (the required accuracy ($DC_{critical}$) is assumed to be equal to 0.999).

On the other hand, an essential question arises after the calculation of the pore size distribution. We do not know how many iterations should be performed by the ASA algorithm in order to obtain a satisfactory PSD curve (i.e., the shape of the PSD does not change significantly during the fitness procedure). Typical plots connecting the CPU time (thus, the number of iterations) and the values of DC are presented in Figures 4 and 5. The increase in the values of DC is very fast. Therefore, DC values close to unity are achieved after performing only several iterations. Moreover, in Figure 5 the comparison between the pore size distributions calculated from the ISHC model for three different values of iterations (20, 41, and 5000, respectively) is shown. It is very interesting that shapes of the PSDs are very similar for a low and high number of iterations (41 and 5000, respectively). Summing up, after several iterations the ASA procedure (the analysis

(41) (a) Terzyk, A. P.; Gauden, P. A.; Kowalczyk, P. *Carbon* **2002**, *40*, 2879. (b) Kowalczyk, P.; Solarz, L.; Terzyk, A. P.; Gauden, P. A.; Gun'ko, V. *Shedae Informaticae*, in press. (c) Kowalczyk, P.; Terzyk, A. P.; Gauden, P. A.; Leboda, R.; Szmechtig-Gauden, E.; Rychlicki, G.; Ryu, Z.; Rong, H. *Carbon* **2003**, *41*, 1113. (d) Kowalczyk, P.; Gun'ko, V. M.; Terzyk, A. P.; Gauden, P. A.; Rong, H.; Ryu, Z.; Do, D. D. *Appl. Surf. Sci.* **2003**, *206*, 67. (e) Kowalczyk, P.; Terzyk, A. P.; Gauden P. A.; Gun'ko, V. M. *J. Colloid Interface Sci.* **2002**, *256*, 378. (f) Gun'ko, V. M.; Leboda, R.; Skubiszewska-Zięba, J.; Turov, V. V.; Kowalczyk, P. *Langmuir* **2001**, *17*, 3148.

(42) (a) Gauden, P. A.; Terzyk, A. P.; Szmechtig-Gauden, E.; Duber, S.; Buczkowski, R.; Kowalczyk, P. *Carbon*, submitted. (b) Szmechtig-Gauden, E.; Buczkowski, R.; Terzyk, A. P.; Gauden, P. A. *Ochrona Środowiska*, in press, in Polish.

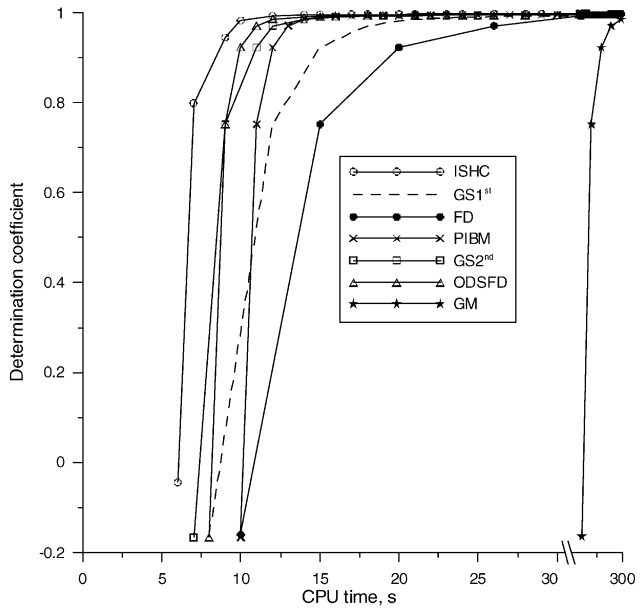

Figure 4. The relation between the values of the determination coefficient DC (thus, the number of iterations) and the CPU time for the system investigated in Table 1 and Figure 3.

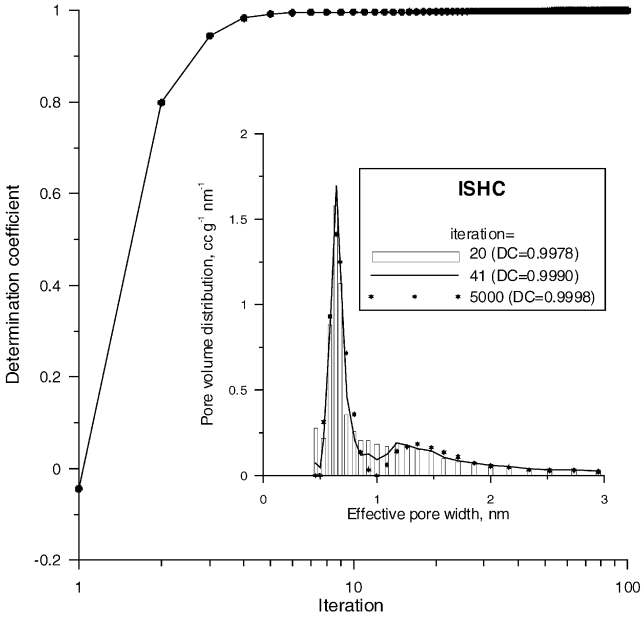

Figure 5. The relation between the values of the determination coefficient DC and the number of iterations. The inset figure shows the comparison of the pore size distributions evaluated for three different numbers of iterations. The calculations were performed by applying the ASA algorithm with the ISHC method for the low-temperature nitrogen adsorption isotherm measured on the activated carbon Norit ROW 0.8 SUPRA.

of the experimental data) can be stopped and the evaluated differential pore size distribution is acceptable and gives sufficient information about the structural heterogeneity of the investigated adsorbent.

Summing up this part, the ISHC and PIMB procedures are faster and more efficient than the others. Therefore, ISHC is chosen arbitrarily in the considerations presented below.

2. Reconstruction of the Differential Pore Size Distribution. In the present study, we use computer experiments (based on the principles outlined below) to study physical adsorption on activated carbons possessing slitlike pores. The properties of the ASA algorithm were investigated assuming the following conditions: nitrogen is the adsorbate; the temperature is taken as equal to 77.5 K (the low-temperature nitrogen adsorption data have been recommended as a typical experiment for characterizing the porosity of adsorbents).[43] In the current study, the activated carbon is assumed to be the adsorbent. The maximal effective slit half-width (H_{max}) is equal to 2 nm (the upper limit of micropore diameters recommended by IUPAC). We decided to take into account the above-mentioned value of H_{max} in order to simplify the considerations; however, the same results can be obtained for wider pores (i.e., the mesoporous adsorbents). The adsorbate has a specified size, and therefore, the minimal effective slit width ($H_{min} = 0.46$ nm) should be larger than the collision diameter of nitrogen ($\sigma_{ff} = 0.3798$ nm). The adsorption isotherms were generated over the relative pressure range from 1×10^{-6} up to $0.9998 p/p_s$ (the number of points equally spaced along $\log(p/p_s)$ is equal to 100). Developed previously, the Nguyen−Do model[32,40,41] (eq 12) is chosen for generating the local adsorption isotherms in order to investigate the stability of the newly proposed ASA algorithm (eqs 7−9).

As mentioned by Rudziński and Everett,[5] real heterogeneous solids can be characterized by a pretty complicated form of the PSD, with a number of local minima and maxima. However, in the structure of some adsorbents (for example, as investigated by us previously,[44] carbonaceous films obtained by Zawadzki and co-workers[45]) the majority of micropores possess the same diameter (a very narrow distribution of pores). On the other hand, the real PSD curve can be (for practical purposes) approximated, with a certain degree of accuracy, by some "smoothing" functions and their plot is described by a small number of parameters.[5−13,46] Therefore, three forms of the postulated monomodal PSD function (eqs 15−17; Figure 6) and three multipeak PSDs (eqs 18−20; Figure 7) are considered below.

1. The Dirac Delta Function.

$$f(H) = \delta(H - H_D) \tag{15}$$

where $\delta(H - H_D) \neq 0$ if $H = H_D$, and $\delta(H - H_D)$ is equal to 0 for $H \neq H_D$. In the current study, the peak is located arbitrarily at $H_D = 1.22$ nm.

2. The Uniform Distribution.

$$f(H) = \chi(H_l) \tag{16}$$

where $\chi(H_l)$ is equal to the same nonzero value of the PSD in the interval $H_l \in \langle H_{min}, H_{max} \rangle$ and $\chi(H_l)$ is equal to 0 for $H_l \notin \langle H_{min}, H_{max} \rangle$. In the current study, the uniform values of the PSD are generated for H_l [nm] $\in \langle 0.958, 1.471 \rangle$.

3. The Gaussian Distribution.

$$f(H) = \exp\left[-\frac{(H - H_0)^2}{2\Delta^2}\right] \tag{17}$$

where H_0 and Δ are the parameters of the PSD function

(43) Sing, K. S. W.; Everett, D. H.; Haul, R. A. W.; Moscou, L.; Pierotti, R. A.; Rouquerol, J.; Siemieniewska, T. *Pure Appl. Chem.* **1985**, *57*, 603.
(44) Terzyk, A. P.; Gauden, P. A.; Zawadzki, J.; Rychlicki, G.; Wiśniewski, M.; Kowalczyk, P. *J. Colloid Interface Sci.* **2001**, *243*, 183.
(45) Zawadzki, J.; Wiśniewski, M.; Weber, J.; Heintz, O.; Azambre, B. *Carbon* **2001**, *39*, 187.
(46) (a) Gauden, P. A. Theoretical Description of the Structural and Energetic Heterogeneity of Carbonaceous Materials. Thesis, N. Copernicus University, Toruń, 2001 (in Polish). (b) Gauden, P. A.; Terzyk, A. P. *J. Colloid Interface Sci.* **2000**, *227*, 482. (c) Gauden, P. A.; Terzyk, A. P. *Theory of Adsorption in Micropores of Carbonaceous Materials*; WICHiR: Warsaw, 2002 (in Polish).

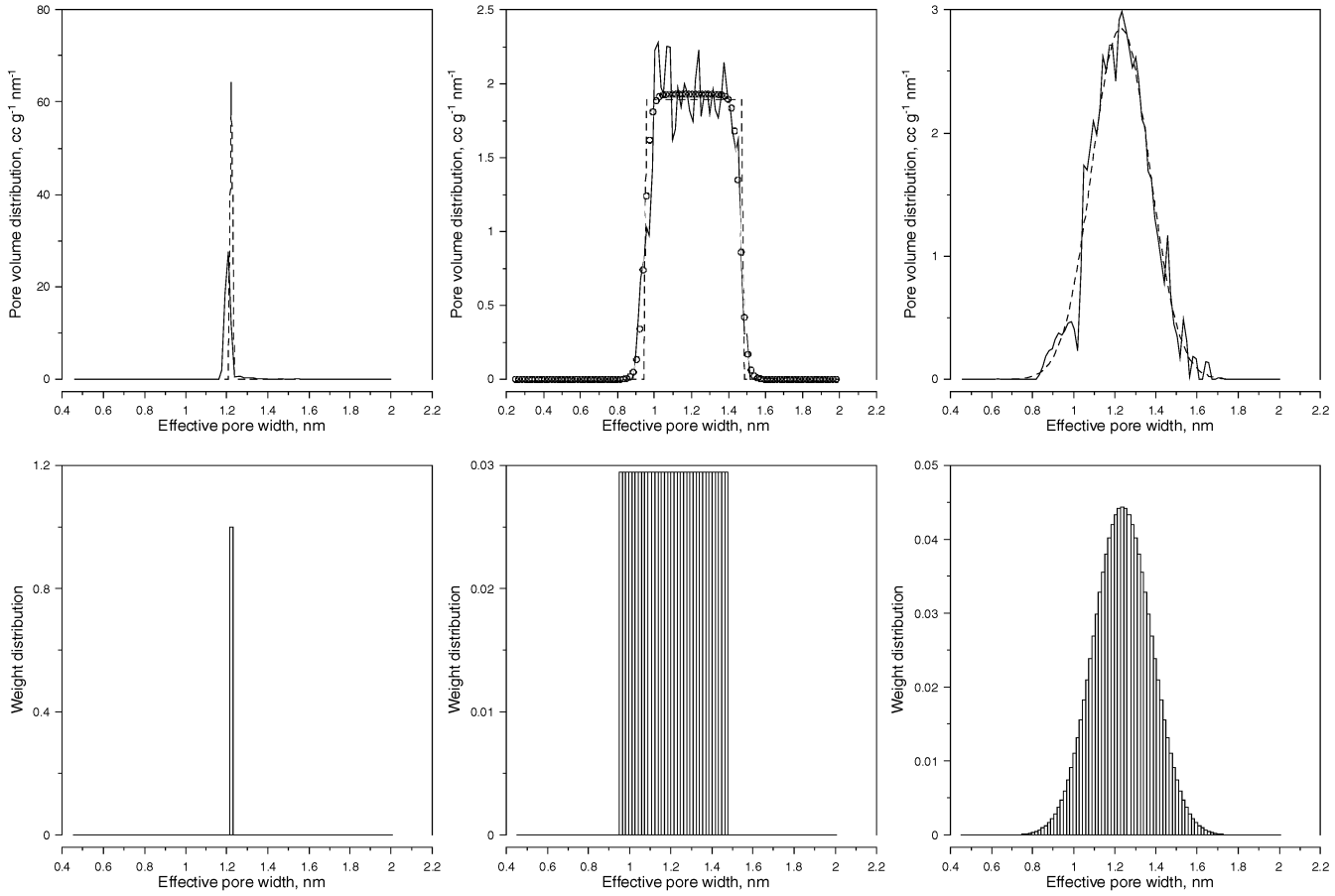

Figure 6. Upper panel: the recovering results (solid lines) of the starting monomodal PSD function of different types (dashed lines) generated based on eqs 15−17. The cumulative symmetric double sigmoidal (SDSCum) function is additionally applied for a uniform PSD (open circles). Lower panel: assumed distributions of weights applied for the generating of isotherms.

characterizing the position of the maximum (the average value) of the PSD and the dispersion (the width of the distribution), respectively. In this study, the values $H_0 = 1.23$ nm and $\Delta = 0.07$ nm are assumed.

4. The Bi-Lorentzian Function.

$$f(H) = \sum_{j=1}^{2} \frac{2A_j}{\pi} \frac{\Delta_j}{4(H + H_{c,j})^2 + \Delta_j^2} \qquad (18)$$

where H_c, Δ, and A are the parameters of the above-mentioned distribution function characterizing the position of the maximum of the PSD, the dispersion (the width of the distribution), and the area, respectively. In the current study, we assumed $H_{c,1} = 0.9$ nm, $H_{c,2} = 1.5$ nm, $\Delta_1 = 0.1$ nm, $\Delta_2 = 0.2$ nm, $A_1 = 0.2$ nm^2, and $A_2 = 0.1$ nm^2.

5. The Tri-Gaussian Distribution.

$$f(H) = \sum_{j=1}^{3} \Lambda_j \frac{1}{\Delta_j \sqrt{2\pi}} \exp\left[- \frac{(H - H_{0,j})^2}{2\Delta_j^2} \right] \qquad (19)$$

where H_0, Δ, and Λ are the parameters of the above-mentioned distribution function characterizing the positions of the maximum of the PSD, the dispersion (the width of the distribution), and the weight of the jth peak, respectively. In the current study, we assumed the following values of parameters: $H_{0,1} = 0.66$ nm, $H_{0,2} = 0.86$ nm, $H_{0,3} = 1.26$ nm, $\Delta_1 = \Delta_2 = 0.015$ nm, $\Delta_3 = 0.1$ nm, $\Lambda_1 = \Lambda_2 = 0.005$, and $\Lambda_3 = 0.9$.

6. The Four-Peak Dirac Delta Function.

$$f(H) = \sum_{j=1}^{4} \delta(H - H_{D,j}) \qquad (20)$$

where $\delta(H - H_{D,j})$ gives the nonzero values of the PSD function if $H = H_{D,j}$, and $\delta(H - H_{D,j})$ are equal to 0 for $H \neq H_{D,j}$. The peaks are localized at 0.770, 1.097, 1.423, and 1.750 nm, respectively.

All the above analyzed differential pore size distribution functions (eqs 15−17) are plotted in Figures 6 and 7. On the basis of the relationships presented in the Appendix, the starting weight distributions are evaluated and the respective plots are also shown in both figures (obviously the condition of the sum of weights being equal to unity is fulfilled; therefore, the theoretical PSDs need not be normalized (see the Appendix) due to the condition of the normalization to unity of all weights). Next, the so-called global adsorption isotherms (eq 12) are generated using 100 Nguyen−Do local adsorption isotherms and applying the above-considered pore size distribution functions (and/or normalizing to unity the distribution of weights). The analyzed range of microporosity is equally divided into 100 subranges. Then, the ASA algorithm is applied for reconstructing modeled differential pore size distributions. During the fitting procedure, the same local adsorption isotherms are used. The algorithm stops when the required accuracy is achieved (the value of the determination coefficient is ≥ 0.9999). Finally, the weight vector is evaluated and on the basis of weights the PSD is calculated using the relationships presented in the Appendix.

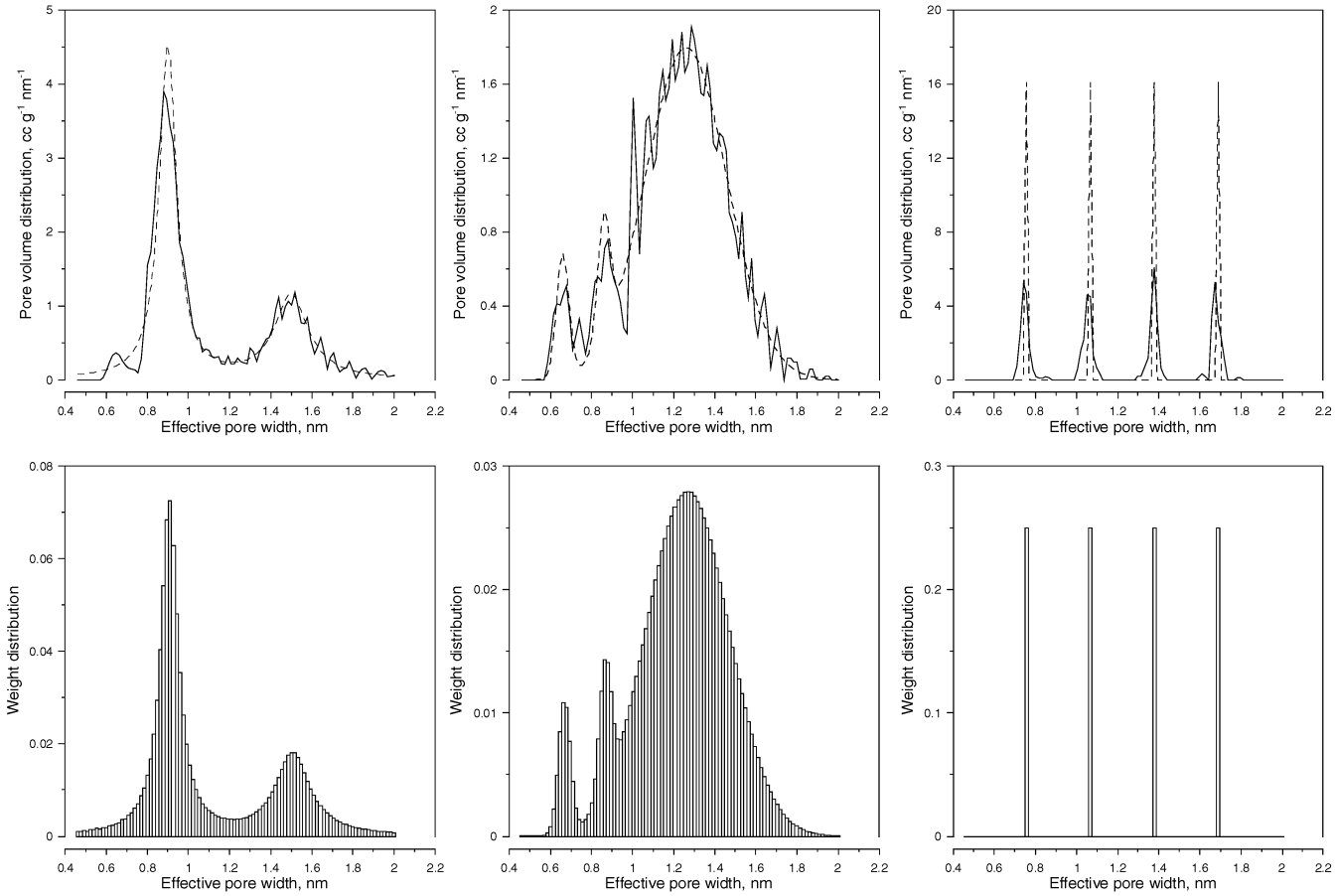

Figure 7. Upper panel: the recovering results (solid lines) of the starting polymodal PSD function of different types (dashed lines) generated based on eqs 18−20. Lower panel: assumed distributions of weights applied for the generating of isotherms.

We want to underline that to test the power of the ASA package some nontrivial continuous and discontinuous functions were applied. The Dirac delta function (Figure 6) is calculated for the peak located at $H_D = 1.22$ nm (i.e., only one local adsorption isotherm is generated), but the recovery procedure is used over a wide range of the effective pore widths ($H \in \langle 0.46, 2 \rangle$). The only noticeable change in the calculated distribution is a small broadening and reduction of the maximum value of the PSD (due to the normalization condition of the weights). This is caused by an infinitely small probability of the evaluation of weights being equal to zero (see eq 11) for the values of the micropore widths different from $H_D = 1.22$ nm. Summing up, the recovery of the original Dirac delta distribution is satisfactory.

Figure 6 also shows the results of recovering the uniform distribution function. In this case, the recalculated PSD is a sharply oscillating function (it contains many small peaks). This is probably caused by the similarity of the local adsorption isotherms (the shapes and the values). Therefore, some weights corresponding to local adsorption isotherms are overestimated, and some of them are underestimated. To eliminate this shortcoming, the cumulative pore size distribution can be described by a smoothing function. Therefore, in this case we applied a cumulative symmetric double sigmoidal (SDSCum) function in order to describe the pore size distribution. This smoothing procedure can be justified due to the high fitness (equal to 0.99996) of the theoretical and generated data. After the smoothing procedure of the cumulative PSD, the ASA gives an acceptable recovery (Figure 6). This result confirms the well-known principle that small differences between neighboring weights can generate significant variations in the differential PSD curve.[18]

For the other studied cases, the shapes of the considered PSDs are quite well reproduced without any assumptions concerning the plots of the examined functions (see the Gaussian function (Figure 6) and the multimodal ones (Figure 7)). Furthermore, the ASA package copes very well with the functions consisting of more than one peak (despite the discontinuous character of some examined functions). Additionally, the ASA algorithm slightly smoothes the shapes of some examined functions (for instance, the Dirac delta function (the first case presented above) and the PSD generated as the sum of four "Dirac delta functions" (the sixth case presented above)). Finally, the functions described by eqs 18−20 have more realistic shapes since in practice many physical processes lead to similar distributions. The models used by us can successfully approximate the Gaussian or similar distributions. Summing up, the ASA is a very powerful package and it can be successfully applied for predicting the pore size distribution of microporous and mesoporous adsorbents.

3. The Influence of Random Noise on the Stability of the Solution of the Inverse Problem. The computational procedure is carried out as follows. The analysis is limited to the fourth case of the above-mentioned PSDs (the bi-Lorentzian function, eq 18), and the assumed $f(H)$ is treated as the reference one. This case is chosen since for carbons and carbonaceous materials it is postulated that the PSD is usually bimodal, that is, pores are grouped

around two diameters.[40−42,45−48] The local adsorption isotherms are calculated according to the Nguyen−Do model (eq 12). Summing up, the global adsorption isotherms (Θ^{theor}) are determined based on eq 7. The random noise is added to the "error-free" simulated data[31,41e] (treated in this case as experimental ones) as shown below:

$$\Theta^{exper}\ (\equiv\Psi_t(p_j)) = (\sum_{i=1}^{N} w_i\Theta_{ND}(p_j,H_i))(1 + 0.01\nu\sigma) = \Theta^{theor}(1 + 0.01\nu\sigma) \quad (21)$$

where Θ^{exper} (see $\Psi_t(p)$ in eqs 7−9) are "noisy" data; ν presents the pseudo-random numbers distributed evenly over the interval (−1,1) (Gaussian noise[34,35,39]); σ is the percentage of "smearing" of the simulated values Θ^{theor}. The random noise procedure is treated as a standard method for investigating the stability of the solution of the inverse problem.[21,23,31,41e,49] On the other hand, this test leads to some pitfalls. First, it is very difficult to evaluate the "true" and maximum values of the percentage of smearing. Second, for a higher disturbance of "measured experimental" data the smoothing procedures before the theoretical description are often used. The procedures are widely applied by different authors, for example, before the calculation of the differential distributions characterizing the energetic and/or geometric heterogeneity of a solid. Moreover, the methods of noising the data sometimes lead to unrealistic results if they are compared to experimental ones. It is obvious that for experimentally measured isotherm data, an increase in relative pressure should be connected with a constant or increasing adsorption value.[10] On the other hand, the disturbing procedure gives unphysical points; that is, sometimes adsorption decreases with a rise in pressure. Regardless of those obvious limitations, this type of calculation gives important information about the stability of the solution of the inverse problem.

Therefore, two cases are investigated in this part. A constant value of the percentage error for all adsorption isotherm data is assumed. The generated global adsorption isotherms (Θ^{theor}) are perturbed by three different noise levels (1, 3, and 5%, Figure 8), a constant percentage level for the whole isotherm. In the second case, the logarithmic relationship between σ (the parameter of eq 21) and Θ^{theor} is analyzed (the low-pressure data are "measured" with a larger error than the data approaching unity),

$$\sigma = \sigma_{sh} - \sigma_{up}\log(\Theta^{theor}) \quad (22)$$

where σ_{sh} is the "shift" value introduced in order to calculate the error for $\Theta^{theor} = 1$ and σ_{up} is the parameter describing the decrease of σ. Thus, the final form of eq 21 is the following:

$$\Theta^{exper} = \Theta^{theor}(1 + 0.01\nu(\sigma_{sh} - \sigma_{up}\log(\Theta^{theor}))) \quad (23)$$

In the current study, three sets of the parameters are assumed ($\sigma_{sh,1} = \sigma_{sh,2} = \sigma_{sh,3} = 0.1\%$, $\sigma_{up,1} = 2.86\%$, $\sigma_{up,2} = 10\%$, and $\sigma_{up,3} = 40\%$), Figure 9. The largest values of the σ_{upper} parameter are hardly likely (a larger noise level than 5% is not observed for measurements performed on modern adsorption apparatus (for example ASAP, Micromeritics[50]), but they are considered to reveal some nuances of the current study.

There is no error imposed on the relative pressure terms. Noisy data (Θ^{exper}) are substituted to the minimization of the functional defined by eq 9. Thus, the approximated solution of $f(H)$ is searched. Next, the approximated solution (calculated from the nitrogen adsorption data disturbed with Gaussian noise) is compared with the postulated PSD function.

The influence of the noise level (a constant value of σ is assumed, eq 21) in the Θ^{theor} data on the behavior of the reconstructed PSD is shown in Figure 8. As shown in this figure, the first node is practically unchanged, contrary to the second one. If the simulated isotherm is perturbed by 3 and 5% noise levels, the reconstructed PSDs are different from the starting ones. Some additional peaks are observed. Thus, the results of the computation show that the accuracy of the input data must be large and/or they should be smoothed if one wishes to solve the given problem successfully. Summing up, the calculation of the PSD for the larger value of σ is close to the edge of the boundary of stability−instability of the solution.[21,23,31,49]

In the second case (eqs 22 and 23), the logarithmic relationship between σ and Θ^{theor} is analyzed (the low-pressure data are "measured" with a larger error than the data approaching unity), Figure 9. It follows from analyzing the results of the reconstructed bimodal distribution that a worse coincidence between the postulated PSD and the reconstructed one is observed if the value of the error significantly increases ($\sigma \approx 70\%$) for adsorption data determined at lower adsorption values. However, these errors do not play a visible role in the reconstruction of the bimodal distribution (especially for the first node) but cause worse resolution in the reconstruction of the bimodal PSD with the largest noisiness of the simulated data. It is not expected (for the case $\sigma_{upper} = 10\%$) that reconstructed results are practically invariable if the data are perturbed by the decreasing percentage noise level.

Summing up, for the case of the simulated "ideal" isotherms (without error), the investigated ASA algorithm reproduced the original bi-Lorentzian distribution with excellent accuracy. For the model adsorption isotherms perturbed by normally distributed errors (σ equal to 1% and σ_{up} equal to 2.86 or 10%, respectively), the distribution $f(H)$ is reproduced well. For larger errors (both investigated relationships between Θ^{theor} and σ), some additional peaks are observed and the obtained PSD curves should be treated with caution.

Therefore, for the data measured with a large error, the application of the smoothing procedure makes the solution seeking easier, and a good coincidence between the postulated and reconstructed data is achieved at the same time. This is shown in Figure 10 where we present the recovery data for the curve disturbed with 10% error (eq 21) after smoothing the noisy data with a Chebyshev polynomial function order 11.

4. The Influence of the Choice of Algorithm (ASA, CONTIN, INTEG) on the Obtained Results. In the presented studies, besides the Norit ROW 0.8 SUPRA carbon described above three samples of activated carbons are additionally investigated to test the proposed ASA algorithm:

(i) $C_{ox}Pt$. A carbonaceous film obtained from cellulose by the method published by Zawadzki[44,45] possessing pores where it was shown (for example from the shape of a high-

(47) Kowalczyk, P.; Terzyk, A. P.; Gauden, P. A. *Langmuir* **2002**, *18*, 5406.

(48) (a) Ismadji, S.; Bhatia, S. K. *Langmuir* **2000**, *16*, 9303. (b) Ismadji, S.; Bhatia, S. K. *Langmuir* **2001**, *17*, 1489.

(49) Jaroniec, M.; Brauer, P. *Surf. Sci. Rep.* **1986**, *65*, 65.

(50) Webb, P. A.; Orr, C. *Analytical Methods in Fine Particles Technology*; Micromeritics Instrument Corp.: Norcross, GA, 1997.

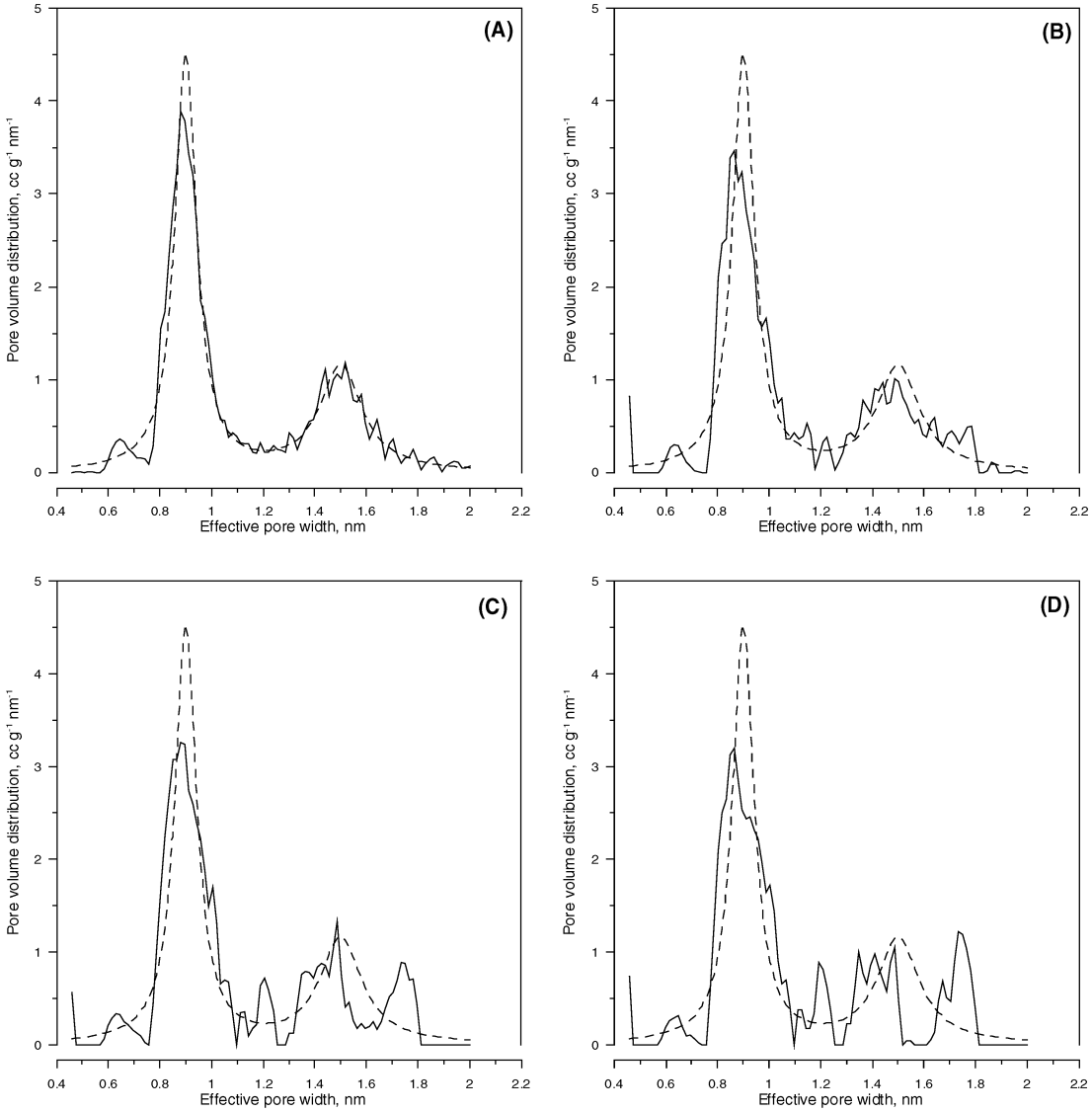

Figure 8. PSDs reproduced from the theoretical simulated adsorption isotherms disturbed with random errors equal to 0, 1, 3, and 5% (eq 21) (solid lines) in comparison to the postulated PSDs (dashed lines).

resolution α_s plot) that the primary micropore filling process predominates.

(ii) Carbon A. A polymeric carbon obtained from poly(furfuryl alcohol) carbonized in a vacuum.[51] A negligibly small concentration of oxygen groups on the surface of this carbon is present, and micropores predominate in the structure (i.e., the "external" surface is negligibly small compared to the apparent surface area of micropores). However, the microporosity is dispersed over a relatively wide range.[46a,c]

(iii) D43/1. (Carbo-Tech, Essen, Germany) A commercial material possessing mainly micropores in the structure; however, the amount of mesopores cannot be neglected.[52]

For the computation of the PSDs of the studied carbons, we have chosen not only the ASA algorithm but two numerical algorithms widely used for the characterization of geometric heterogeneity of adsorbents, namely, CONTIN[24,47,53] and INTEG.[21,50] For the INTEG algorithm, the local isotherms are generated basing on the density functional theory (DFT). The PSD curve is evaluated using DFT PLUS software for the regularization parameter equal to $\lambda = 0.00001$ (ASAP 2010, Micromeritics).[50] The differential PSD for the tested activated carbon obtained by means of Provencher's regularization procedure (CONTIN) of solving the global adsorption isotherm with the Nguyen and Do kernel is shown.

The PSDs of some of the tested carbon materials are shown in Figure 11. The figures in the lower panel show the fit of isotherms calculated based on the ASA method to the experimental ones (the fit for other methods was

(51) (a) Rychlicki, G.; Terzyk, A. P. *Adsorpt. Sci. Technol.* **1998**, *16*, 641. (b) Terzyk, A. P.; Rychlicki, G. *Adsorpt. Sci. Technol.* **1999**, *17*, 323. (c) Rychlicki, G. *The Influence of the Chemical Nature of Surface of the Carbon on the Adsorption and Catalytic Processes*; N. Copernicus University: Toruń, 1989 (in Polish).

(52) (a) Terzyk, A. P. *Adsorpt. Sci. Technol.* **1999**, *17*, 441. (b) Terzyk, A. P.; Rychlicki, G. *Colloids Surf., A* **2000**, *163*, 135. (c) Terzyk, A. P. *Adsorpt. Sci. Technol.* **2000**, *18*, 477. (d) Terzyk, A. P. *J. Colloid Interface Sci.* **2000**, *230*, 219. (e) Terzyk, A. P. *Colloids Surf., A* **2001**, *177*, 23. (f) Terzyk, A. P. *J. Colloid Interface Sci.* **2002**, *247*, 507 (g) Terzyk, A. P.; Gauden, P. A. *Sep. Sci. Technol.* **2001**, *36*, 513. (h) Terzyk, A. P.; Gauden, P. A. *J. Colloid Interface Sci.* **2002**, *249*, 256. (i) Terzyk, A. P.; Rychlicki, G.; Biniak, S.; Łukaszewicz, J. P. *J. Colloid Interface Sci.* **2003**, *257*, 13.

(53) (a) Gun'ko, V. M.; Leboda, R.; Marciniak, M.; Grzegorczyk, W.; Skubiszewska-Zięba, J.; Malygin, A. A.; Malkov, A. A. *Langmuir* **2000**, *16*, 3227. (b) Puziy, A. M.; Matynia, T.; Gawdzik, B.; Poddubnaya, O. I. *Langmuir* **1999**, *15*, 6016. (c) Gun'ko, V. M.; Do, D. D. *Colloids Surf., A* **2001**, *193*, 71.

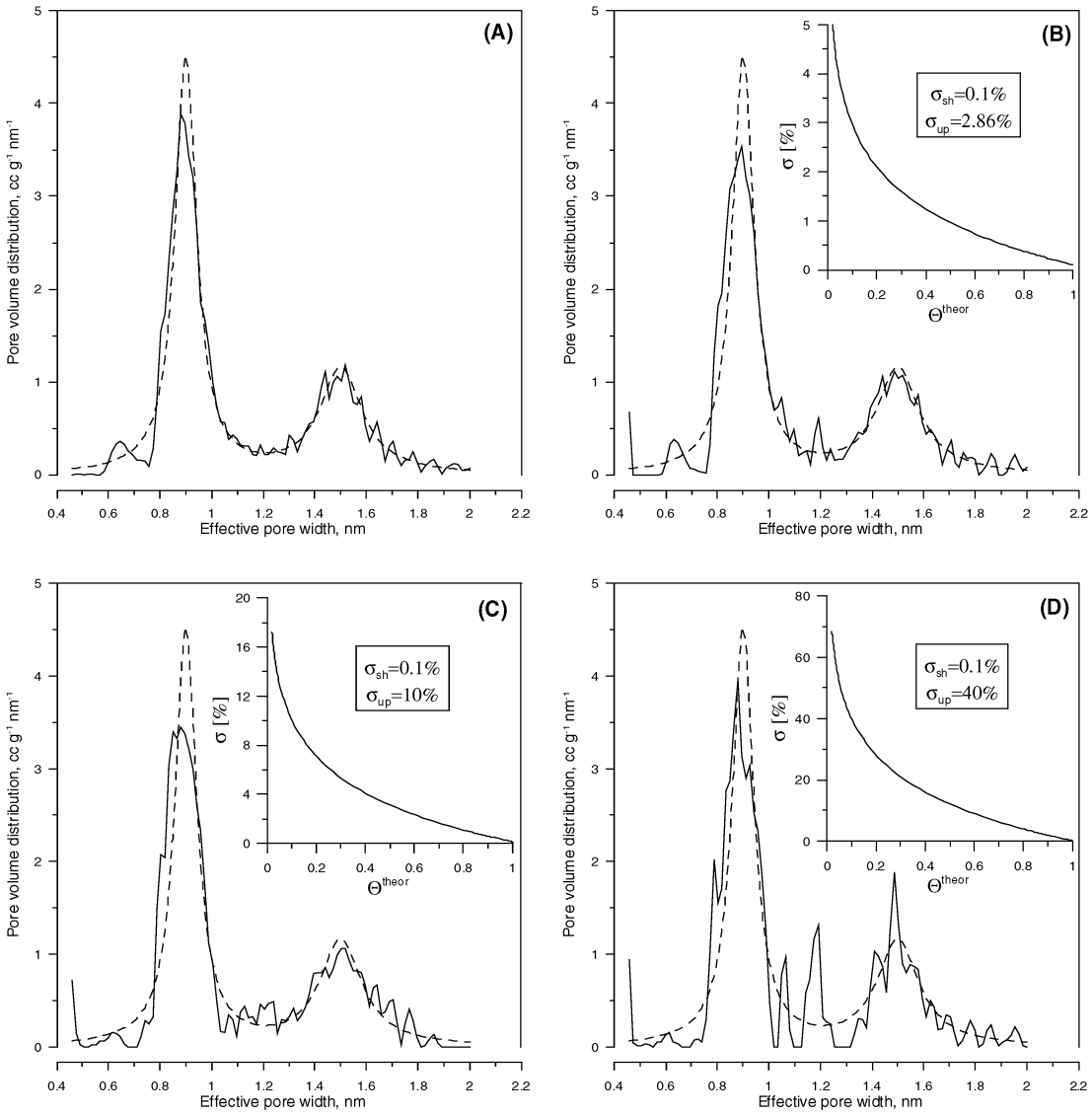

Figure 9. PSDs reproduced from the theoretical simulated adsorption isotherms disturbed with decreasing random errors (eq 23) (solid lines) in comparison to the postulated PSDs (dashed lines). The inset figures show the logarithmic relationship between σ and Θ^{theor} (eq 22).

also very good (see Figure 12) and is omitted in this figure for clarity of presentation). The CONTIN algorithm gives a similar range of PSDs for the investigated adsorbent as compared to others (ASA and/or INTEG), but the peaks are usually slightly shifted to larger or smaller effective pore widths. Moreover, our recent results indicate that this procedure gives similar PSD plots for carbonaceous materials possessing a significantly different pore structure.[41b] This indicates the low sensitivity of this method. On the other hand, the two remaining tested algorithms show the differences in the shapes of the PSDs for the same carbons. The carbonaceous film prepared by Zawadzki is characterized by a very small dispersion of micropores (i.e., high homogeneity of internal structure). The bimodal character of the PSD is observed for all investigated samples. For this group, the ND method leads to DC values close to 0.95, while the values from the DFT method are close to 0.99. In this case, the largest differences between the values of DC calculated for both methods are observed (however, both methods describe experimental isotherms satisfactorily). The widening of the distribution of microporosity does not change the above situation; that is, the DFT method still leads to a better fit than the ND method does, and the differences in the values of DC are around 0.03 (carbon A and Norit ROW 0.8 SUPRA). If mesoporosity appears on the PSD curve, the differences between the goodness of the fit achieved from the two methods vanish, and the DFT and ND methods lead practically to the same PSD curves (D43/1).

Figure 12 shows the fit of theoretical isotherms to experimental data for the carbon Norit ROW 0.8 SUPRA. In the case of the DFT method, the influence of the parameter λ is also shown. Recently this method has been treated as one of the most advanced, standard, and widely recommended procedures. However, there are two main problems associated with the application of the INTEG algorithm. The first, associated with the DFT method, is the choice of this so-called regularization parameter, λ. The regularization parameter describes the weighting of "the adsorption" and "experimental error". Therefore, the selection of this parameter plays a central role in finding the solution. Von Szombathely and co-workers[21] distinguished two principally different ways for the best choice: the manual choice by interactive judgment of the solution on a graphic displayed for several values of λ (applied in DFT PLUS software (INTEG algorithm)) or the postula-

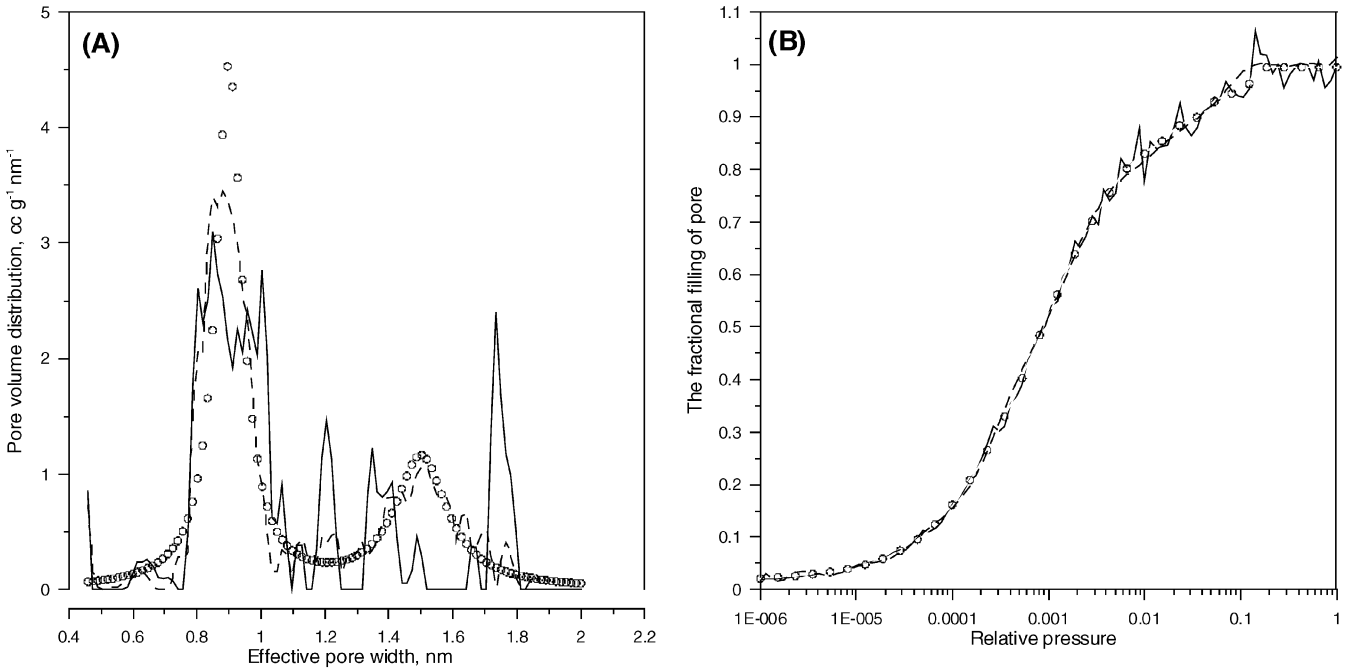

Figure 10. PSDs reproduced from the theoretical simulated adsorption isotherm (open points, for clarity of presentation only 33% of the points are shown) disturbed with a random error equal to 10% (eq 21) (solid line) and next, evaluated from the disturbed isotherm after smoothing by a Chebyshev polynomial (dashed line).

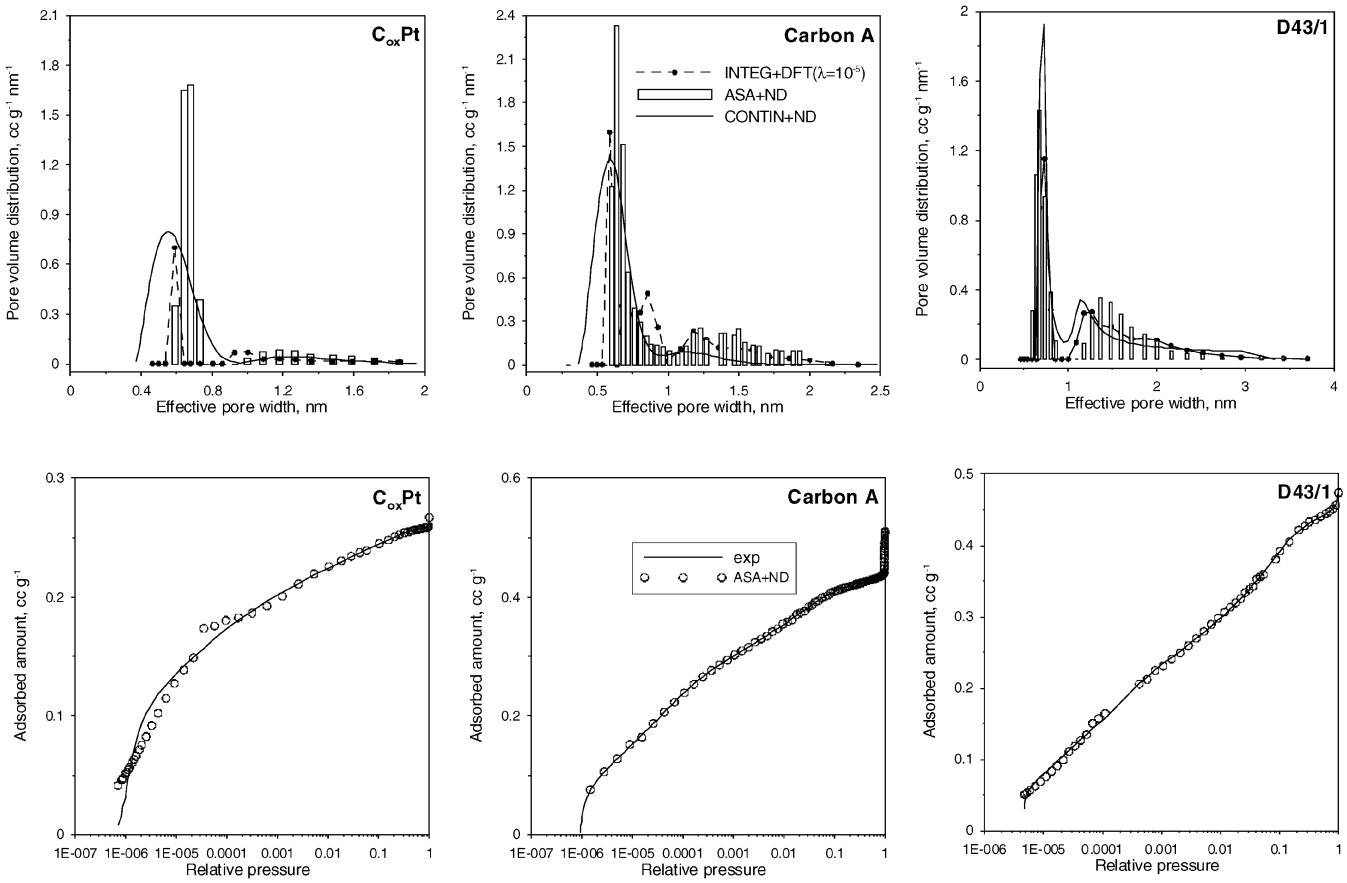

Figure 11. Upper panel: PSDs of studied carbons calculated by applying different methods described in the text. Lower panel: the fit of the ND and ASA methods to the experimental data.

tion of an aim function for the appropriate optimal regularization parameter λ_{opt}, the choice of which can be automated by suitable search algorithms (for example in the CONTIN package[53c]). The first procedure is investigated for the INTEG algorithm in the current paper. Figure 13 shows the comparison of the pore size distributions obtained from the DFT method for different values of λ. It can be noticed that the similarity between the INTEG and ASA methods is observed for very small values of λ (a very small "experimental" error is assumed).

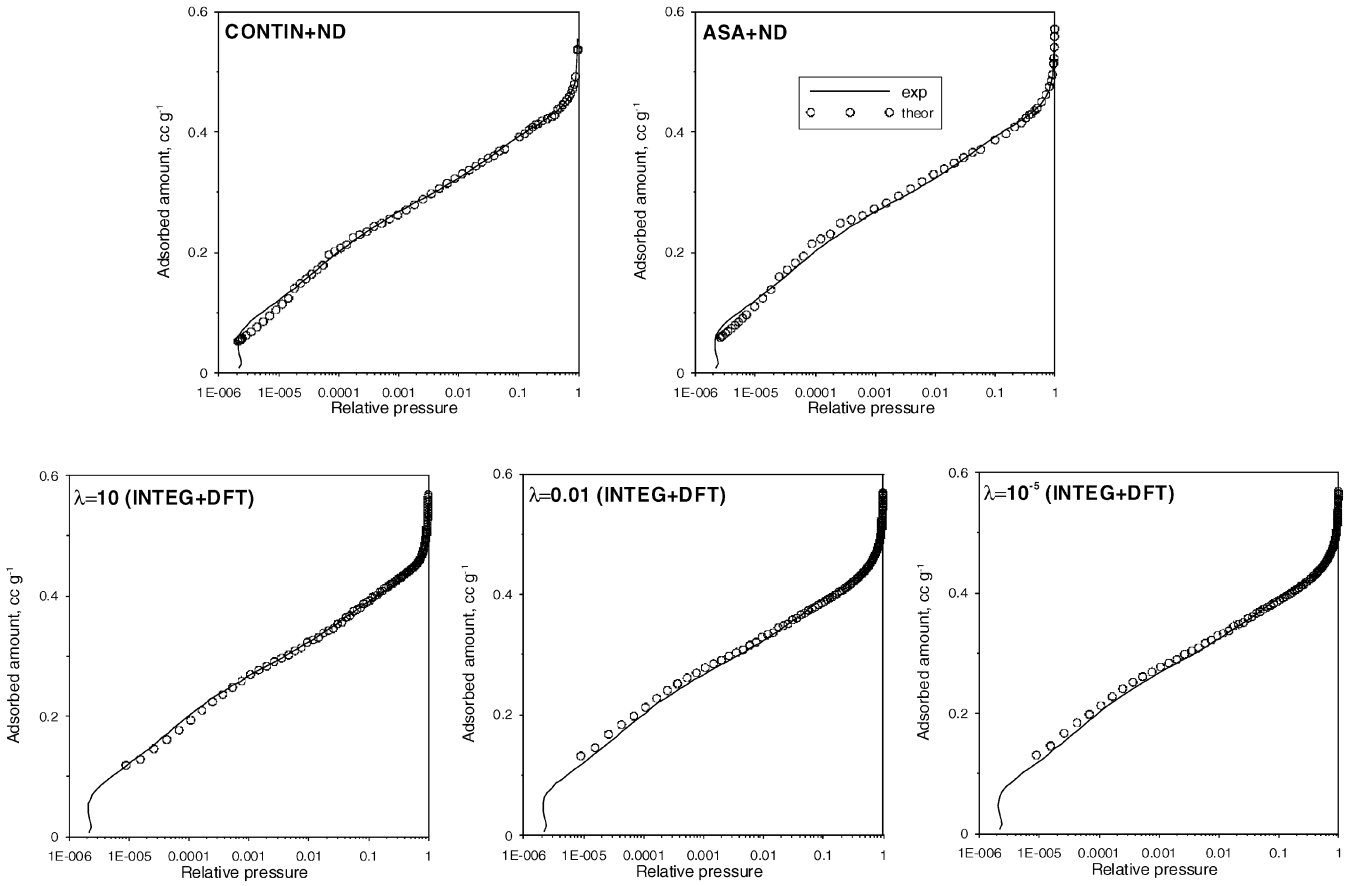

Figure 12. The fit of the tested methods to experimental nitrogen adsorption data (77.5 K) determined for carbon Norit ROW 0.8 SUPRA. For other studied adsorbents, a similar fit was obtained.

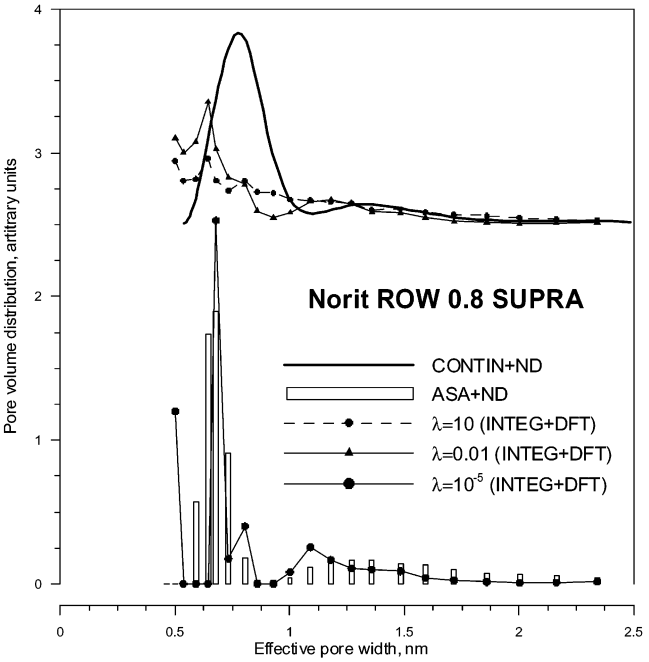

Figure 13. Pore size distributions of activated carbon Norit ROW 0.8 SUPRA obtained using the INTEG algorithm (DFT Plus software) for different values of smoothing parameter λ, ASA, and CONTIN algorithms with the Nguyen−Do method of calculation of the local adsorption isotherms.

Moreover, Figure 13 shows that the pore size distribution becomes successively flatter as the effective smoothing parameter increases. The same results were obtained by Davies and Seaton.[54] The PSD shape changes from initial polymodal distributions to much flatter monomodal ones. Summing up, the influence of the parameter λ is the most important; therefore, to compare both methods we assumed $\lambda = 0.00001$.

V. Conclusions

The methods based on the assumption that the pore structure is characterized by a (known a priori) multipeak distribution function are very popular.[5−13,55] Different distributions may be used to study the heterogeneity of solids (for example, gamma-type, Gaussian, log-normal, Maxwell−Boltzmann, exponential higher-degree polynomial, and others). However, from a practical point of view, the methods that do not introduce the assumptions connected with the shape of the energy (and/or pore size) distribution function are more interesting and important than those discussed above.[5,6,12,56]

For example, Seaton et al.[57] used a multilinear least-squares fitting of the parameters of the assumed PSD function so as to match measured isotherm data. A similar method was employed by Lastoskie et al.[58] in their analysis

(54) Davies, G. M.; Seaton, N. A. *Carbon* **1998**, *36*, 1473.
(55) (a) *Adsorption*: *Theory, Modeling, and Analysis*; Toth, J., Ed.; Surfactant Science Series, Vol. 107; Marcel Dekker: New York, 2002; p 175. (b) Scaife, S.; Kluson, P.; Quirke, N. *J. Phys. Chem. B* **2000**, *104*, 313. (c) Sweatman, M. B.; Quirke, N. *J. Phys. Chem. B* **2001**, *105*, 1403.
(56) (a) Borówko, M. Adsorption on Heterogeneous Surfaces. In *Adsorption*: *Theory, Modeling, and Analysis*; Toth, J., Ed.; Surfactant Science Series, Vol. 107; Marcel Dekker: New York, 2002; p 105. (b) Rege, A. U.; Yang, R. T. Models for the Pore-Size Distribution of Microporous Materials from a Single Adsorption Isotherm. In *Adsorption*: *Theory, Modeling, and Analysis*; Toth, J., Ed.; Surfactant Science Series, Vol. 107; Marcel Dekker: New York, 2002; p 175.
(57) Seaton, N. A.; Walton, J. P. R. B.; Quirke, N. *Carbon* **1989**, *27*, 853.

using the nonlocal functional theory (NL-DFT). Later, an important contribution toward the numerical deconvolution of the distribution result was made by Olivier and co-workers.[50] They developed a program based on the regularization method called INTEG,[21] in which no restrictions were imposed on the form of the PSD. Moreover, this method was found to be numerically complicated. On the other hand, the CONTIN package and/or the Tikhonov regularization method are also successfully used for the estimation the pore size distribution of adsorbents.[24,47,53,59] Also, a simpler optimization technique has recently been suggested by Nguyen and Do.[32]

However, the calculation of the local adsorption isotherms and the determination of the PSD are two independent objects of studies. Once a set of molecular simulations have been conducted for a given adsorbate in a set of model pores of a given type of sorbent material, the PSD can be determined relatively quickly for any microporous material with nearly similar structural characteristics. The availability of commercial software packages for performing molecular simulations for a variety of applications has made such methods increasingly attractive as the reference methods to test the prediction of other proposed adsorption theories. In the past decade, two main methods based on statistical mechanics have emerged. These are the DFT and the molecular simulation methods such as grand-canonical Monte Carlo (GCMC) simulations. Both of them are steadily gaining popularity for PSD estimation and are widely discussed in the literature. The DFT method provides a practical alternative to more accurate but computationally intensive methods such as molecular simulation. However, certain drawbacks of the method have to be taken into account. Lastoskie et al.[58] have summarized some of these limitations. One practical problem, which is more of an experimental error than a flaw in the actual method, is the unreliability of isotherm data in the very low pressure range. The lowest relative pressure of the measured isotherm dictates the lower bound of the PSD calculation beyond which it needs to be truncated. Frequently, the experimental isotherms are improperly equilibrated due to diffusional limitations at low temperatures, which can result in the underestimation of the PSD in the micropore range. Taking into account all mentioned and other (the accurate estimation of the sorbate−sorbate−sorbent interaction, the pore connectivity aspects, the thermodynamic verifications) limitations further complicates the DFT calculations. The greater accuracy of the prediction (molecular simulation techniques) is, of course, at the cost of considerably more calculation time than for methods such as DFT.

As mentioned above, sometimes the numerical solution of the integral equation by means of some programs has been carried out without any assumptions for the shape of the evaluating distribution function. However, this procedure can lead to some artifacts; for example, negative parts in the PSD plot are possible.[21,60] They fail to possess any physical meaning, but if the distribution is dominated by the negative parts, then this is a strong hint that the local model does not appropriately describe the experimental data. In the proposed numerical ASA algorithm, no assumptions about the form of the reconstructed function are made but the negative parts of the calculated distributions were not achieved. The iteration in the ASA algorithm is carried out using the non-negativity constraints on the vector solution (no adjusting parameters are assumed to eliminate the negative regions). On the other hand, it is obvious that the values of weights should be greater than zero (or equal to zero), eq 11, since the value of adsorption (local isotherms) from the gaseous phase cannot be negative.

The numerical experiments have shown that the way the initial approximation $f(H)$ is chosen (in the ASA algorithm, the uniform distribution of the weights is assumed) has no influence on the results of the final approximation. In the ASA program, the well-known procedures for estimating the relative minimum in one dimension are used. All minimization routines applied with ASA give very similar values and shapes of the pore size distributions. However, in our opinion the simple iterated hill-climber algorithm is faster and more effective than the others. Moreover, the increase in the value of the determination coefficient is very fast during the fitness procedure. The analysis of the experimental adsorption data shows that after several iterations the ASA can be stopped. Evaluated in this way, the differential PSD is acceptable as long as sufficient information about the structural heterogeneity of the investigated adsorbent is considered.

We want to underline that to test the power of the ASA package some nontrivial continuous and discontinuous functions were applied and they were reconstructed satisfactorily. Moreover, the influence of a random noise on the stability of the solution of the inverse problem was investigated. For low and medium noise levels, the reproducibility of perturbed isotherms was good. Summing up, from this part of the study it is apparent that the generated isotherms ("true" and perturbed) contain full information about the assumed distribution (number of peaks, their location, area, etc.).

To confirm this, the results of the ASA calculations for an experimental isotherm were shown and compared with the PSD evaluated from the INTEG and CONTIN algorithms. The described ASA procedure evaluates the PSD very fast. Moreover, the main advantage of the ASA, comparing the majority of the other known algorithms, is its simplicity. This advantage is very important due to the applicability for a wide group of scientists. In our opinion, this numerical algorithm seems to be a very promising tool for investigating problems connected with solving the Fredholm integral equation of the first type.

Reproducibility of some algorithms is achieved since they try to select the most smooth solution from a great number of those which are evaluated with experimental data. On the other hand, as a rule there is a requirement of a smooth solution for the regularization methods.[15,20−22,61] Therefore, the resolution depends on the experimental error. If a solution (the "true" distibution) is a sharply oscillating function (characterized by many peaks), one should be careful in the interpretation of the evaluated results.[22] An increase of the smoothing (regularization) parameter leads to strong smoothness and disappearance of some (reasonable for experimental studies) peaks in the distribution. So the smoothness of the unknown distribution function $f(y)$ was used as an additional minimizing condition for the stabilization of the solution. Only in the case in which the possibility of smoothness is restricted by a small value of experimental error can one

(58) Lastoskie, C.; Gubbins, K. E.; Quirke, N. *J. Phys. Chem. B* **1993**, *97*, 4786.

(59) (a) Ravikovich, P. I.; Vishnyakov, A.; Russo, R.; Neimark, A. V. *Langmuir* **2000**, *16*, 2311. (b) Gusev, V. Y.; O'Brien, J. A.; Seaton, N. A. *Langmuir* **1997**, *13*, 2815.

(60) (a) Hunger, B.; Matysik, S.; Heuchel, M.; Geidel, E.; Toufar, H. *J. Therm. Anal.* **1997**, *49*, 1997. (b) Hunger, B.; Matysik, S.; Heuchel, M.; Einicke, W.-D. *Langmuir* **1997**, *13*, 6249.

(61) Mamleev, V. Sh.; Bekturov, E. A. *Langmuir* **1996**, *12*, 3630.

proceed to the physical interpretation of the PSD (the CONTIN and INTEG algorithms). On the other hand, the same tendency is observed for the ASA algorithm.

Summing up, the proposed ASA algorithm is faster and simpler than projected by others and can be successfully applied for the calculation of the pore size as well as the energy distribution of solids. The continuous pore size distribution can be considered as a discrete PSD because the representation of a narrow peak in the form of the delta Dirac function does not lead to an appreciable accuracy loss.[22,61] It is assumed that real solids are characterized by a discrete distribution function depicting the PSD as a set of sharp and narrow peaks.

VI. Appendix

Simulated starting and reconstructed isotherms were calculated based on the assumed (the ideal shape) or evaluated distribution functions, $f(z)$. Therefore, the weight of a local function $g_{\text{theor}}(z,p)$ (see eq 7) can be calculated using the following relationship (moreover, with the fulfillment of the normalization condition):

$$w_i = 0 \qquad \text{if } f(z_i) = 0 \tag{A}$$

for arbitrary weights (i.e., $1 \le i \le N$). On the other hand, if $f(z_i) \neq 0$ the values of the weight vector can be calculated based on

$$w_{i,1} = \left(\frac{f(z_{i,1})}{\Psi_{\text{t,max}}}\right)(z_{i,1} - z_{i,2}) \tag{B}$$

for the first nonzero value of the distribution function,

$$w_i = \left|\frac{2f(z_i)}{\Psi_{\text{t,max}}} - \frac{w_{i+1}}{z_{i+1} - z_i}\right|(z_i - z_{i-1}) \tag{C}$$

for $1 < i < N$, and

$$w_{i,N} = \left(\frac{f(z_{i,n})}{\Psi_{\text{t,max}}}\right)(z_{i,N} - z_{i,N-1}) \tag{D}$$

for the last nonzero value of the distribution function.

On the other hand, based on the optimized values of the weight vector $\bar{\mathbf{w}}$ the recalculated and/or solved distribution function, $f(z)$, can be generated from the following relationships for $w_i = 0$:

$$f(z_i) = 0 \qquad \text{if } w_i = 0 \tag{E}$$

for arbitrary weights (i.e., $1 \le i \le N$). On the other hand, if $w_i \neq 0$ the values of the weight vector can be calculated based on

$$f(z_{i,1}) = \Psi_{\text{t,max}}\left(\frac{w_{i,1}}{z_{i,2} - z_{i,1}}\right) \qquad \text{for } i = 1 \tag{F}$$

for the first nonzero value of weight,

$$f(z_i) = \Psi_{\text{t,max}}\left(0.5\left|\frac{w_i}{z_i - z_{i-1}} + \frac{w_{i+1}}{z_{i+1} - z_i}\right|\right) \tag{G}$$

for $1 < i < N$, and

$$f(z_{i,N}) = \Psi_{\text{t,max}}\left(\frac{w_{i,N}}{z_{i,N} - z_{i,N-1}}\right) \tag{H}$$

for the last nonzero value of the distribution function.

LA0270441